EXPLOITING SERUM INTERACTIONS WITH CATIONIC BIOMATERIALS ENABLES LABEL-FREE CIRCULATING TUMOR CELL ISOLATION

A Thesis

Presented to the Faculty of the Graduate School

of Cornell University

In Partial Fulfillment of the Requirements for the Degree of

Master of Science

by

Carlos Castellanos

January 2017

ABSTRACT

Herein we investigate the role charged biomaterials and fluid properties have on microfluidic capture and isolation of circulating tumor cells. We determine that heparan sulfate proteoglycans on cancer cell surfaces are responsible for elevated electric charge of cancer cells compared with white blood cells and that these proteoglycans help mediate adhesive interactions between cells and charged surfaces in albumin-containing fluids. Cancer cell firm adhesion to charged surfaces persists when cells are bathed in up to 1% (w/v) human albumin solution, while white blood cell adhesion is nearly abrogated. As many protocols rely on electrical interactions between cells and biomaterials, our study could reveal a new determinant of efficient adhesion and targeting of specific tissue types in the context of a biological fluid environment.

Carlos Alfonso Castellanos was born in New Orleans, Louisiana in 1985. In 2012 Carlos graduated Magna Cum Laude with a B.S. in Biochemistry from Arizona State University. During his undergraduate studies, Carlos worked to control enzyme position and orientation on surfaces with the objective of performing surface-bound, multi-protein reactions with enhanced efficiencies similar to reaction pathways in biological systems. Carlos joined Professor Mike King's research group at Cornell University in Ithaca, NY in late 2012 for advanced study in Biomedical Engineering.

I wish to thank the Meinig School of Biomedical Engineering and the Graduate School of Cornell University for the financing, facilities, and faculty which have made available a remarkable educational opportunity. I wish to give particular thanks to Professor M.R. King who has served as chairman of my advisory committee and who unfailingly showed personal and professional interest in the student as well as the study.

TABLE OF CONTENT

CHAPTER 1

SURFACTANT FUNCTIONALIZATION INDUCES ROBUST, DIFFERENTIAL ADHESION OF TUMOR CELLS AND BLOOD CELLS TO CHARGED NANOTUBE-COATED BIOMATERIALS UNDER FLOW

1.1 Abstract

The metastatic spread of cancer cells from the primary tumor to distant sites leads to a poor prognosis in cancers originating from multiple organs. Increasing evidence has linked selectin-based adhesion between circulating tumor cells (CTCs) and endothelial cells of the microvasculature to metastatic dissemination, in a manner similar to leukocyte adhesion during inflammation. Functionalized biomaterial surfaces hold promise as a diagnostic tool to separate CTCs and potentially treat metastasis, utilizing antibody and selectin-mediated interactions for cell capture under flow. However, capture at high purity levels is challenged by the fact that CTCs and leukocytes both possess selectin ligands. Here, a straightforward technique to functionalize and alter the charge of naturally occurring halloysite nanotubes using surfactants is reported to induce robust, differential adhesion of tumor cells and blood cells to nanotube-coated surfaces under flow. Negatively charged sodium dodecanoate-functionalized nanotubes simultaneously enhanced tumor cell capture while negating leukocyte adhesion, both in the presence and absence of adhesion proteins, and can be utilized to isolate circulating tumor cells regardless of biomarker expression. Conversely, diminishing nanotube charge via functionalization with decyltrimethylammonium bromide both abolished tumor cell capture while promoting leukocyte adhesion.
[1]

[1] The content of this chapter was published as a research article:
Michael J. Mitchell*, Carlos A. Castellanos*, Michael R. King, "Surfactant Functionalization Induces Robust, Differential Adhesion of Tumor Cells and Blood Cells to Charged Nanotube-Coated Biomaterials Under Flow," *Biomaterials,* 56:179-186(2015).
***Authors contributed equally to this work.**
M.J.M., C.A.C., and M.R.K. conceived of research; M.J.M., C.A.C., and M.R.K. designed research; M.J.M. and C.A.C. performed research; M.J.M. and C.A.C. analyzed data; M.J.M., C.A.C., and M.R.K. wrote the paper.

1.2 Introduction

Metastasis, the spread of cancer cells from a primary tumor to anatomically distant organs, contributes to over 90% of cancer- related deaths [1]. Cancer cells shed from the primary tumor, which can number as many as one million cells per gram of tumor per day [2,3], enter the bloodstream as circulating tumor cells (CTCs) via the process of intravasation [4,5]. Once in blood, CTCs must withstand fluid shear forces and immunological stress to translocate to microvessels in anatomically distant organs [6,7]. CTCs adhesively interact with receptors on the endothelial cell wall under flow, in a manner similar to the leukocyte adhesion cascade involved in inflammation and lymphocyte homing to lymphatic tissues [8,9]. Recent work has shown that CTCs display glycosylated ligands similar to leukocytes, which can trigger the initial adhesion with selectin receptors on the endothelium [10,11]. Due to their rapid, force-dependent binding kinetics, selectins can initiate CTC rolling adhesion along the blood vessel wall [12,13]. CTCs transition from rolling to eventual firm adhesion, allowing for transmigration into tissues and the formation of secondary tumors [14]. While surgery, radiation, and chemotherapy have proven generally successful at treating primary tumors that do not invade the basement membrane, the difficulty of detecting distant micrometastases has made the majority of metastatic cancer treatments ineffective. As a means to combat metastasis, approaches are currently being explored to target and kill CTCs in the bloodstream before the formation of secondary tumors [15-18]. Additionally, methods are being developed to isolate CTCs at high purity levels from patient blood, for the development of personalized medicine regimens for those with metastatic cancer [19-21].

CTCs are sparsely distributed in the bloodstream, with CTC concentrations as low as 1-100 cells/mL [22]. Their separation and isolation from blood is commonly referred to as a “needle in a haystack problem”, as leukocytes and erythrocytes are present in concentrations of

one million and one billion cells per milliliter of blood, respectively [7,23]. Thus, numerous techniques for CTC isolation are in development, including magnetic bead-based CTC separation assays [24], flow-based microfluidic platforms for rapid isolation of CTCs from whole blood [25,26], and devices to separate tumor cells based on their chemotactic phenotype [27]. Our lab has recently developed microscale flow devices that mimic the metastatic adhesion cascade process to capture and separate CTCs from whole blood under flow conditions. Utilizing surfaces coated with recombinant human E-selectin (ES) and antibodies against the CTC markers epithelial cell adhesion molecule (EpCAM) and prostate-specific membrane antigen (PSMA), we have fabricated flow devices to rapidly separate viable CTCs from patient blood and deliver targeted chemotherapeutics to cancer cells [26,28]. However, improvement of current CTC isolation purity levels is challenged by the fact that both CTCs and leukocytes express ES ligands [8].

Halloysite nanotubes (HNT) are naturally occurring clay minerals that are typically 800 ± 300 nm in length, 50 ± 70 nm in outer diameter, and 10 ± 30 nm in inner diameter [29]. Halloysite ($Al_2Si_2O_5(OH)_4$) is a two-layered (1:1) aluminosilicate that consists of an external siloxane (SieOeSi) surface and an internal aluminol (AleOH) surface [30]. At physiological pH, HNT has a negatively charged outer surface and a positively charged inner lumen [31], which has been exploited for the encapsulation and sustained release of drugs such as Nifedipine, Furosemide, and dexamethasone [32]. The differences in HNT surface charge have also been exploited for the selective adsorption of anionic and cationic surfactants, which significantly alters HNT zeta potential [33]. Our lab has shown that HNT-coated biomaterials of nanoscale roughness can increase surface area and thus selectin protein adsorption [34], which can enhance selectin-mediated cancer cell capture. Herein, we present the use of HNT in combination with

cationic and anionic surfactants to develop nanostructured biomaterials that differentially adhere tumor cells and leukocytes under flow conditions.

1.3 Materials and Methods

1.3.1 Cell culture

Human colon adenocarcinoma COLO 205 (ATCC #CCL-222), breast adenocarcinoma MCF7 (ATCC #HTB-22), and breast adenocarcinoma MDA-MB-231 (ATCC #HTB-26) cell lines were purchased from American Type Culture Collection (ATCC; Manassas, VA, USA). COLO 205 and MDA-MB-231 cells were grown in RPMI 1640 supplemented with 10% fetal bovine serum (FBS) and 1% PenStrep (PS), all purchased from Invitrogen (Grand Island, NY, USA). MCF7 cells were cultured in Eagle's Minimum Essential Medium supplemented with 0.01 mg/mL bovine insulin, 10% FBS, and 1% PenStrep, all purchased from Invitrogen. Both cell lines were incubated under humidified conditions at 37°C and 5% CO2, and were not allowed to exceed 90% confluence. In preparation for capture assays, cancer cells were removed from culture via treatment with Accutase (SigmaeAldrich, St. Louis, MO, USA) for 10 min prior to handling. All cells were washed in HBSS, and resuspended at a concentration of 1.0×10^6 cells/mL in HBSS flow buffer supplemented with 0.5% HSA, 2 mM $Ca2^+$, and 10 mM HEPES (Invitrogen), buffered to pH 7.4.

1.3.2 Polymorphonuclear (PMN) cell isolation

Human neutrophils were isolated as described previously [35,36]. Human peripheral blood was collected from healthy blood donors via venipuncture after informed consent and stored in heparan containing tubes (BD Biosciences, San Jose, CA, USA). Blood was carefully layered over 1-StepTM Polymorphs (Accurate Chemical and Scientific Corporation, Westbury, NY, USA) and separated via centrifugation using a Marathon 8K centrifuge (Fisher Scientific,

Pittsburgh, PA, USA) at 1800 rpm for 50 min. Polymorphonuclear (PMN) cells, also known as neutrophils, were extracted and washed in cation-free HBSS, and excess red blood cells were lysed hypotonically. Prior to capture assays, neutrophils were resuspended in HBSS flow buffer supplemented with 0.5% human serum albumin (HSA), 2 mM $Ca2^{+}$, and 10 mM HEPES (Invitrogen), buffered to pH 7.4.

1.3.3 Halloysite nanotube functionalization

Halloysite nanotubes (HNT; NaturalNano, Rochester, NY, USA) were added to water to a final concentration of 6.6% (w/v). 1.6 g HNT was added to 100 mL of 0.1 M aqueous sodium dodecanoate (NaL) and 2.4 g HNT were added to 100 mL of 0.1 M aqueous decyl trimethyl ammonium bromide (DTAB; SigmaeAldrich) and mixed using a magnetic stirrer for 48 h. Surfactant-treated nanotubes were then washed several times in water and allowed to dry overnight. Untreated HNT were kept in water at a concentration 6.6% (w/v). NaL and DTAB-treated HNT were stored in water or methanol respectively, to a final concentration of 6.6% (w/v). To evaluate adsorption of surfactants to HNT, the hydrodynamic radius (nm) and zeta potential (mV) of HNT, NaL-HNT, and DTAB-HNT were measured by dynamic light scattering (DLS) using a Malvern Zetasizer Nano ZS (Malvern Instruments Ltd., Worcestershire, UK). Treated and untreated nanotubes at a concentration of 0.37% (w/v) were prepared prior to DLS measurements, using the same solvents as described above for functionalized and untreated HNT samples. To assess the effect of ES adsorption on HNT zeta potential, 0.5 mL of HNT, NaL-HNT, and DTAB-HNT at a concentration of 1.1% (w/v) were centrifuged at 13,000 rpm for 10 min and incubated with 0.5 mL of ES at a concentration of 2.5 mg/mL for 2.5 h at RT. All samples were centrifuged at 13,000 rpm for 10 min and resuspended in water at the same concentration used for HNT measurements in the absence of ES. Colloidal stability of treated

and untreated HNT was assessed by allowing samples of treated and untreated HNT to settle for 24 h after mixing.

1.3.4 Fabrication of nanostructured HNT surfaces

Microrenathane (MRE) tubing (Braintree Scientific, Braintree, MA, USA) of inner diameter 300 mm was cut to 55 cm in length and fastened onto the stage of an Olympus IX-71 inverted microscope (Olympus, Center Valley, PA, USA). Ethanol was rinsed through the tubes using a motorized syringe pump (KDS 230; IITC Life Science, Woodland Hills, CA, USA) at a flow rate of 1 mL/min. To functionalize the inner MRE surface with HNT, microtubes were washed thoroughly with distilled water, followed by incubation with poly-L-lysine solution (0.02% w/v in water) for 5 min and incubation with untreated or NaL-functionalized HNT (NaL-HNT, 1.1% w/ v) for 5 min. To functionalize the surface with DTAB-treated HNT (DTAB-HNT), aqueous 2:8 L-glutamic acid (0.1% w/v, Sigma) was incubated in microtubes for 5 min, prior to incubation with DTAB-HNT (1.1% w/v) for 5 min. Microtubes were then washed thoroughly with distilled water at 0.02 mL/min to remove non-adsorbed halloysite, and cured overnight at room temperature (RT). To immobilize ES adhesion protein to HNT-coated surfaces, recombinant human ES/Fc chimera (rhE/Fc) (R&D Systems, Minneapolis, MN, USA) at a concentration of 2.5 mg/mL was perfused through microtubes at 0.02 mL/min. ES was incubated for 2.5 h at RT within HNT-coated microtubes and smooth microtubes in the absence of HNT. In some experiments, HNT-coated surfaces were utilized in the absence of ES. All surfaces were blocked for nonspecific cell adhesion for 1 h via perfusion and incubation with 5% (w/v) bovine serum albumin (BSA, SigmaeAldrich) at 0.02 mL/ min. ES protein was activated with calcium enriched flow buffer for 5 min prior to cell capture experiments.

1.3.5 ES surface adsorption assay

To characterize ES adsorption on smooth and immobilized HNT surfaces, anti- human CD62E (BD Biosciences, San Jose, California, USA) conjugated to an allophycocyanin (APC) fluorophore was perfused through microtubes at 0.02 mL/min and incubated for 2.5 h at RT, following incubation with ES protein and BSA as described above. Unbound ES antibodies were washed from surfaces using flow buffer. Fluorescent images of adsorbed ES on surfaces were acquired at 90 magnification using an IX-81 inverted microscope linked to a Hitachi CCD camera (Hitachi, Japan). Fluorescent images were analyzed using a three dimensional (3D) surface plot plug-in for ImageJ to obtain pixel intensity data.

1.3.6 HNT surface characterization

To characterize immobilized HNT surfaces, 100 mL of 1.1% untreated HNT, NaL- HNT, and DTAB-HNT solutions were carefully dried on 3 cm x 3 cm polyurethane (PU) sheets (Thermo Scientific, USA) and sputter coated with Au prior to visualization. SEM images of untreated HNT, NaL-HNT, and DTAB-HNT immobilized onto PU surfaces were acquired with the Leica Stereoscan 440 scanning electron microscope (Leica Microsystems Gmbh, Wetzlar, Germany). For atomic force microscopy (AFM) measurements, flat samples of HNT-coated surfaces were prepared on polystyrene microscope slides (Thermo Fisher Scientific, Rochester, NY, USA) using an 8-well flexiPERM gasket (SigmaeAldrich) following the same method used for microtube functionalization. Samples were then imaged using a Veeco DI-3000 AFM (Veeco Instruments, Inc., Woodbury, NY). 10 mm x 10 mm images were recorded at random locations on each sample. Three images each of the flat HNT-coated samples and untreated surfaces were analyzed in WSxM 5.0 software [37] to inspect the surface height profiles and root-mean-square surface roughness.

1.3.7 Cell capture assay

Cell suspensions were perfused through microtubes using a motorized syringe pump and monitored via an inverted microscope linked to a Hitachi CCD KP-M1AN camera (Hitachi, Japan) and a Sony DVD Recorder DVO-1000MD (Sony Electronics Inc., San Diego, California, USA). Cancer cells were perfused at 0.008 mL/min (wall shear stress of 0.5 dyn/cm^2) for 15 min, and then 0.04 mL/min (wall shear stress of 2.5 dyn/cm^2) for 45 min. Polymorphonuclear neutrophils were perfused through microtubes at 0.04 mL/min for 60 min. Mixtures of cancer cells and leukocytes at cancer cell:leukocyte ratios of 1:1 and 1:10 were perfused through microtubes at 0.04 mL/min for 60 min. The number of adhered cells was taken from ten random video frames for each microtube.

1.3.8 Statistical analysis

Data sets were plotted and analyzed using Microsoft Excel (Microsoft, Redmond, WA, USA) and GraphPad Prism 5.0 (GraphPad software, San Diego, CA, USA). All results were reported as the mean ± standard error of the mean (SEM) or standard deviation (SD) as indicated. Two-tailed paired and unpaired t-tests, and one-way ANOVA with Tukey post-tests were utilized for statistical analyses. P-values less than 0.05 were considered significant.

1.4 Results

We are interested in exploiting the negatively charged outer surface and positively charged inner lumen of HNT to alter surface charge via simple surfactant functionalization (Fig. 1A), while maintaining HNT surfaces of nanoscale roughness, to differentially capture cancer cells and blood cells via ES adhesion proteins under flow conditions (Fig. 1B). Due to the negatively charged outer surface and positively charged inner lumen of HNT, we sought to manipulate the nanotube charge using both positive and negatively charged surfactants (Fig. 1A). Sodium dodecanoate (NaL) and decyl trimethyl ammonium bromide (DTAB) were used to

neutralize the positive inner lumen and the negative outer surface charge, respectively (Fig. 1A). NaL and DTAB possess negative and positive functional head groups, respectively, which are needed to bind to the surface and inner lumen of HNT [33]. The aqueous dispersibility of HNT is affected by both hydrophobic interactions and electrostatic effects [33]. Functionalization of HNT by mixing with NaL (NaL-HNT) for 48 h formed stable aqueous dispersions (Fig. 1C), and possessed a negative zeta potential greater than that of untreated HNT (Fig. 1D). These results are consistent with the idea that NaL molecules penetrate within HNT and neutralize the positive charge within the nanotube lumen. Additionally, the increase in negative nanotube charge due to NaL treatment allows the nanotubes to interact with water via charge-dipole interactions.

Conversely, functionalization of HNT with DTAB (DTAB-HNT) via mixing for 48 h diminished the intrinsic negative charge of HNT (Fig. 1D), with polar head groups of DTAB neutralizing external negative charges. At the same time, the long hydrocarbon chain of DTAB is left exposed to solvent water molecules. For DTAB-HNT to disperse in water, non-polar chains must move between water molecules, substituting their weak attractions for strong hydrogen bonds among water molecules [38]. Unable to substitute for intermolecular hydrogen bonds, and aggregating due to hydrophobic forces, DTAB-HNT quickly sediment in a manner similar to untreated HNT (Fig. 1C). Adsorption of ES adhesion receptors to HNT, NaL-HNT, and DTAB-HNT altered charge minimally, by ~2-5 mV (Fig. 1D).

Functionalized HNT can then be immobilized in polyurethane microtubes to create HNT-coated surfaces of nanoscale roughness (Fig. 1B). To evaluate the effect of surfactant treatment on the immobilization of HNT to form surfaces of nanoscale roughness, we characterized both treated and untreated HNT samples immobilized on polyurethane sheets using scanning electron microscopy (SEM). Larger polyurethane sheets were used for analysis rather than microtubes to

minimize sample damage during handling and preparation. Poly-L-lysine (PLL) coatings were used to immobilize HNT and NaL-HNT, with the negatively-charged HNT and NaL-HNT being attracted to the positively-charged PLL coating via electro- static interactions. Conversely, negatively-charged glutamic acid coatings were used to immobilize DTAB-HNT. SEM images revealed that, regardless of surfactant treatment, HNT immobilization creates filamentous surfaces, with HNT protruding from all surfaces (Fig. 1E). AFM images also confirmed that immobilized HNT samples all displayed tubular structures protruding outward from the surfaces at varying feature heights, regardless of surfactant treatment (Fig. 1F, G). Root mean square (RMS) roughness values of all HNT-coated surfaces were within the range of 140-200 nm (Fig. 1H). This range of roughness has previously been shown to enhance cancer cell adhesion via increasing formation of focal adhesion complexes [39]. These data suggest that simple surfactant mixing can functionalize and alter HNT charge, without effecting the immobilization of HNT to create surfaces of nanoscale roughness.

To evaluate the effects of functionalized HNT surfaces (Fig. 2A) on the adsorption of ES receptors, ES was immobilized on smooth, untreated, and treated HNT surfaces and labeled with fluorescent ES antibodies to determine protein fluorescence intensity. Fluorescence micrographs indicated that ES was immobilized on smooth (Fig. 2B), NaL-HNT (Fig. 2C),

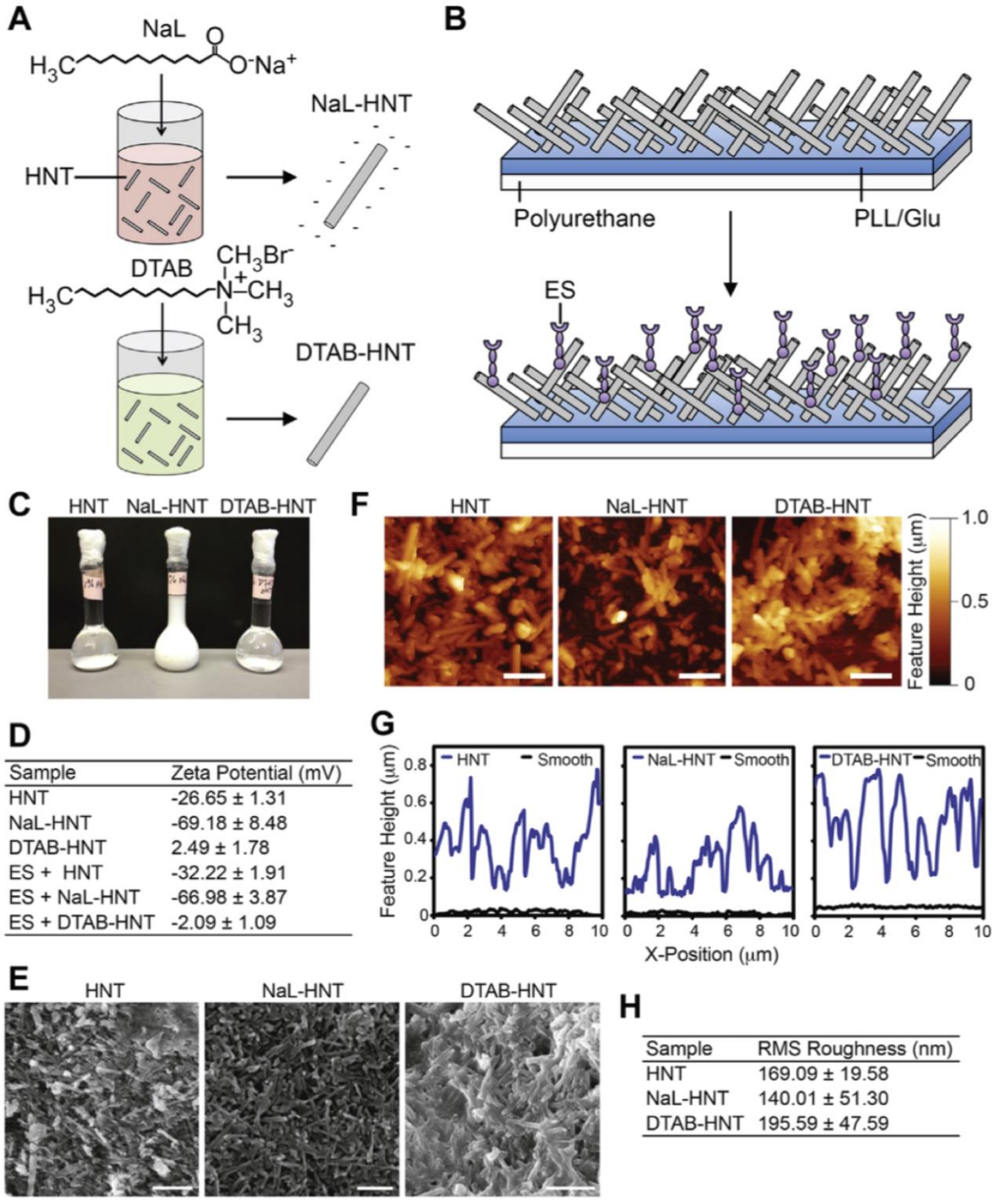

Fig. 1. Functionalization of halloysite nanotubes (HNTs) with surfactants to fabricate nanostructured surfaces of altered surface charge for flow-based cell capture assays. (A) Negative charge of HNT is enhanced via mixing and functionalization with sodium dodecanoate (NaL) surfactant (NaL-HNT). Intrinsic negative charge of HNT is attenuated via hmixing and functionalization of decyltrimethylammonium bromide (DTAB) surfactant (DTAB-HNT). (B) HNTs are immobilized onto polyurethane flow device surfaces coated

with poly-L-lysine (for HNT and NaL-HNT) or glutamic acid (for DTAB-HNT) for cell capture assays. Surfaces can be further functionalized with adhesion proteins, such as E-selectin (ES) to facilitate cell capture. (C) Stability of HNT, NaL-HNT, and DTAB-HNT dispersions (1.1 wt %) 24 h after mixing. (D) Zeta potential (mV) measurements of HNT samples, incubated with and without E-selectin (ES), using dynamic light scattering. Data are presented as the mean ± standard deviation of three independent measurements. (E) SEM images of polyurethane substrates with immobilized HNT samples. Scale bar = 2 μm. (F) AFM images of HNT samples immobilized on polyurethane substrates. Scale bar = 2 μm. (G) Representative surface feature height profiles of HNT samples immobilized onto polyurethane substrates, compared to smooth surfaces. Nanotube profiles have been shifted up by 100 nm for ease of viewing. (H) Root-mean-square (RMS) roughness measurements of HNT surfaces. Data are mean ± standard deviation of three independent measurements.

untreated HNT (Fig. 2D), and DTAB-HNT (Fig. 2E). Quantification of surface fluorescence intensity showed that untreated and treated HNT surfaces increased ES adsorption, with all HNT surfaces possessing significantly greater average ES fluorescence intensities than smooth surfaces (Fig. 2F). Enhanced ES adsorption to HNT surfaces is likely due to the increase in surface area created by HNT immobilization, previously shown by our lab to increase protein adsorption [34]. Differences in ES adsorption on treated and untreated HNT could be due to changes in HNT surface charge, since differences in surface roughness were minimal (Fig. 1H) and thus surface area differences between HNT surfaces are likely negligible. With an isoelectric point at pH 5.2, ES assumes a net negative charge at physiologic pH. Decreased ES adsorption on NaL-HNT compared to other HNT surfaces is thus likely due to electrostatic repulsion between ES and NaL-HNT, both negatively charged. These results indicate that HNT immobilization to biomaterial surfaces enhances ES adsorption.

We then investigated the use of nanostructured surfaces of negatively charged NaL-HNT to facilitate capture of flowing tumor cells and leukocytes via ES-mediated adhesion. Our lab has previously developed reactive biomaterial surfaces that have been utilized for the study of

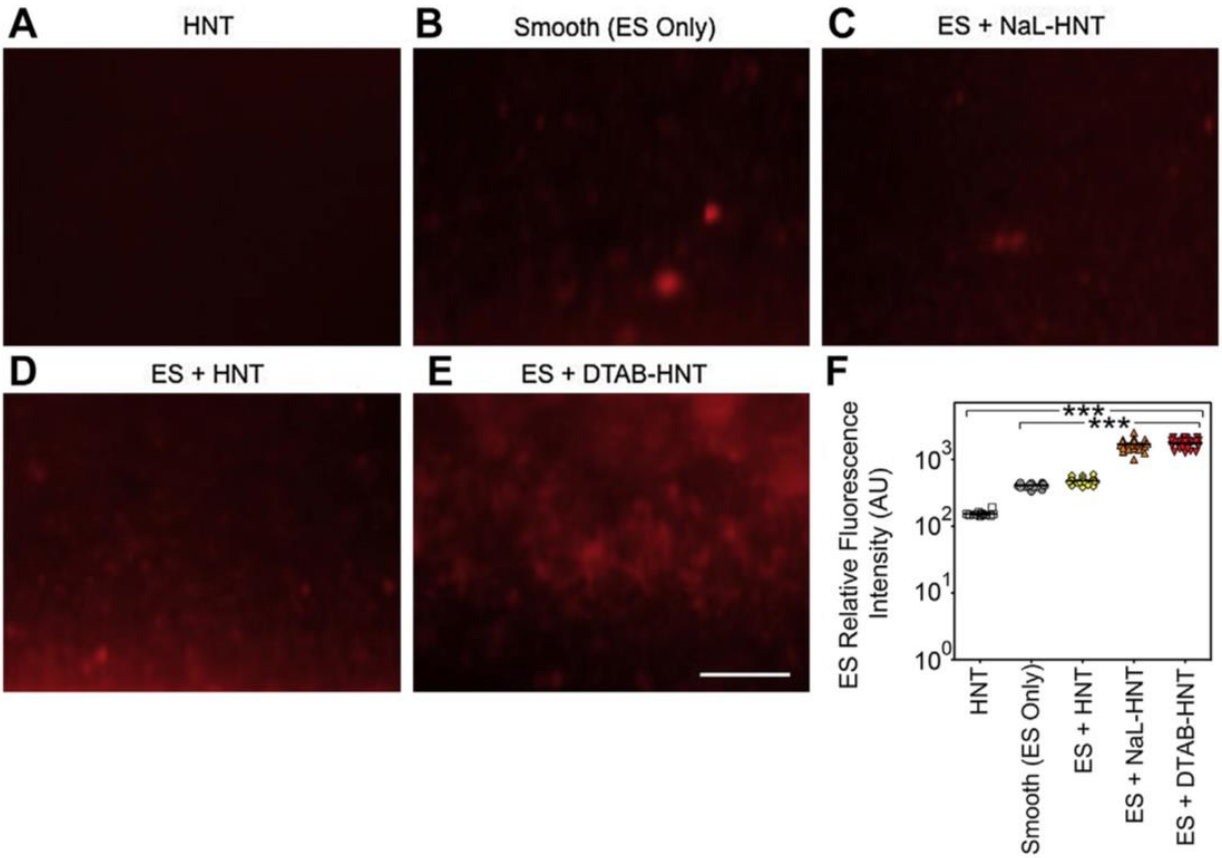

Fig. 2. Detection of immobilized fluorescent ES on biomaterial surfaces. (A-E) Representative high magnification fluorescence micrographs of recombinant human ES (red) adsorbed on immobilized HNT (control without ES; A) surfaces, smooth (ES only; B) surfaces, immobilized NaL-HNT (C), HNT (D), and DTAB-HNT (E) coated biomaterial surfaces. Scale bar = 40 μm. (F) Immobilized ES relative fluorescence intensity values on smooth and nanostructured biomaterial surfaces. Calculated values are mean ± standard deviation (n = 3). Statistics were calculated using a one-way ANOVA with Tukey post test. ***P < 0.0001. (For interpretation of the references to color in this figure legend, the reader is referred to the web version of this article.)

leukocyte, stem cell, and tumor cell adhesive interactions with selectins under flow [13,40,41]. Colorectal adenocarcinoma COLO 205 and breast adenocarcinoma MCF7 cells were used in these experiments as model CTCs because they possess ligands for ES, are known to interact with ES under physiological shear stresses [42,43], and form metastases in vivo [44-46]. As expected, COLO 205 cells adhesively interacted with nanostructured HNT surfaces consisting of immobilized ES (ES þ HNT) under flow (Fig. 3A), at a physiological flow rate of 0.04 mL/min (wall shear stress (WSS) = 2.5 dyn/cm^2). Interestingly, increasing the negative charge of HNT

with NaL surfactant dramatically increased the number of COLO 205 cells recruited via ES under flow (Fig. 3A), compared to untreated HNT-coated surfaces. Enhancement of HNT charge with NaL increased the number of COLO 205 cancer cells captured from flow by ~150%, compared to surfaces comprised of HNT without surfactant treatment (Fig. 3B). Capture of breast MCF7 cancer cells from flow on NaL- HNT surfaces increased by over 800% compared to HNT surfaces without surfactant treatment, demonstrating that this approach can be utilized to target and capture tumor cells from multiple organs (Fig. 3C).

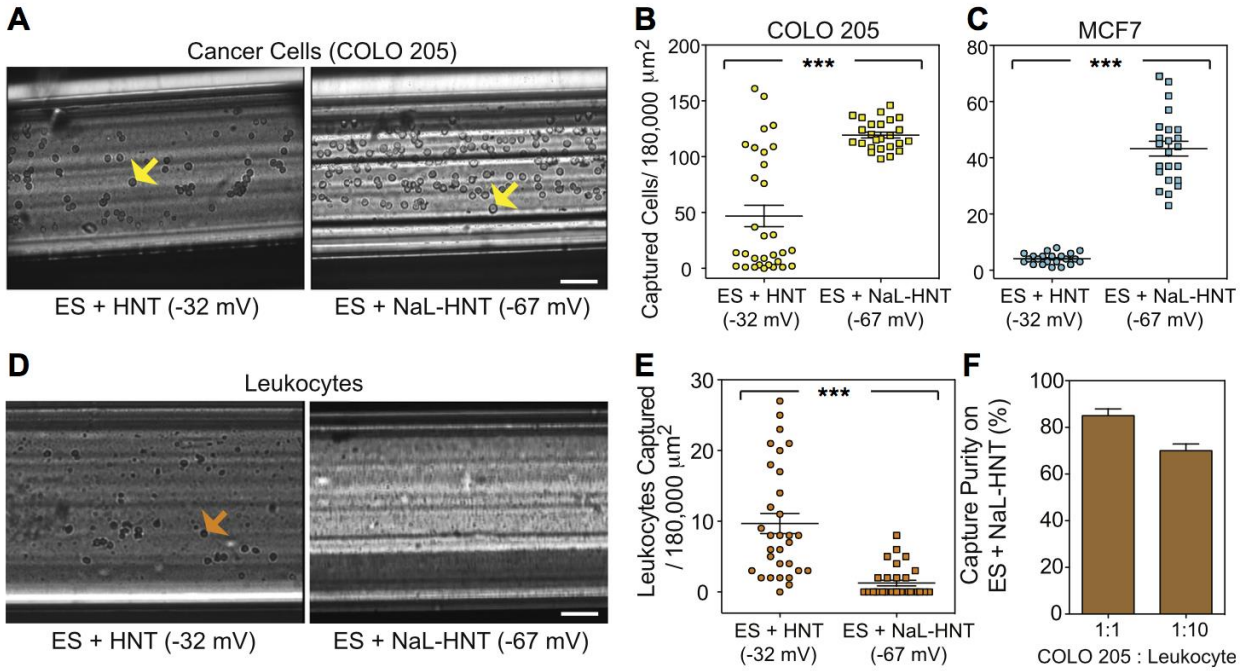

Fig. 3. Negatively charged surfactant-functionalized HNT simultaneously enhance cancer cell capture while eliminating leukocyte adhesion. (A) E-selectin (ES)-mediated adhesion of colorectal adenocarcinoma COLO 205 cells under flow over surfaces coated with ES + HNT and ES + NaL-HNT. Yellow arrows denote adhered COLO 205 cells. Scale bar = 100 µm. (B, C) Number of captured COLO 205 (B) and breast adenocarcinoma MCF7 (C) cells per 180,000 µm^2. n = 20 or more image frames analyzed for each condition. Statistics calculated using a two-tailed unpaired t-test. ***P < 0.0001. (D) ES-mediated adhesion of primary human leukocytes under flow over surfaces coated with ES + HNT and ES + NaL-HNT. Orange arrows denote adhered neutrophils. Scale bar = 50 µm. (E) Number of captured leukocytes per 180,000 µm^2. Calculated values are mean ± SEM. n = 20 or more image frames analyzed for each condition. Statistics calculated using a two-tailed unpaired t-test. ***P < 0.0001. (F) Purity (%) of COLO 205 cancer cells captured from a mixture of cancer cells and leukocytes at COLO 205:leukocyte ratios of 1:1 and 1:10. (For

interpretation of the references to color in this figure legend, the reader is referred to the web version of this article.)

Approximately 1 CTC is present for every one million leukocytes in a given patient blood sample, and CTCs and leukocytes both possess similar ligands for ES. However, enhancement of HNT charge with NaL had the opposite effect on leukocyte adhesion to ES. While flowing leukocytes readily adhered to surfaces consisting of ES and HNT in the absence of surfactant (flow rate = 0.04 mL/ min, WSS 1⁄4 2.5 dyn/cm^2), nearly all adhesion was abolished upon enhancing HNT charge with NaL (Fig. 3D). The number of flowing leukocytes captured from flow decreased by over 90% on NaL-HNT surfaces, compared to surfaces consisting of HNT without surfac- tant treatment (Fig. 3E). We then performed an initial assessment of the purity of flowing cancer cells captured from a mixture of both COLO 205 cancer cells and leukocytes (flow rate = 0.04 mL/min, WSS = 2.5 dyn/cm^2), with COLO 205:leukocyte ratios of 1:1 and 1:10. Purities as high as 90% and 75%, or enrichments as high as four- and twenty-fold, were achieved upon perfusion of cell mix- tures of 1:1 and 1:10, respectively, over HNT surfaces with enhanced negative charge (Fig. 3F). Overall, these data suggest that alteration of HNT charge with NaL can induce a robust response to both enhance cancer cell capture and diminish leukocyte adhesion, both in isolation and in mixtures of cancer cells and leukocytes of varying ratios.

To assess if ES-mediated cancer cell capture and leukocyte repulsion on nanostructured surfaces is dependent on HNT charge, we functionalized HNT with DTAB surfactant to abolish the intrinsic negative charge of HNT (Fig. 1A, D). Upon perfusion of COLO 205 cells at

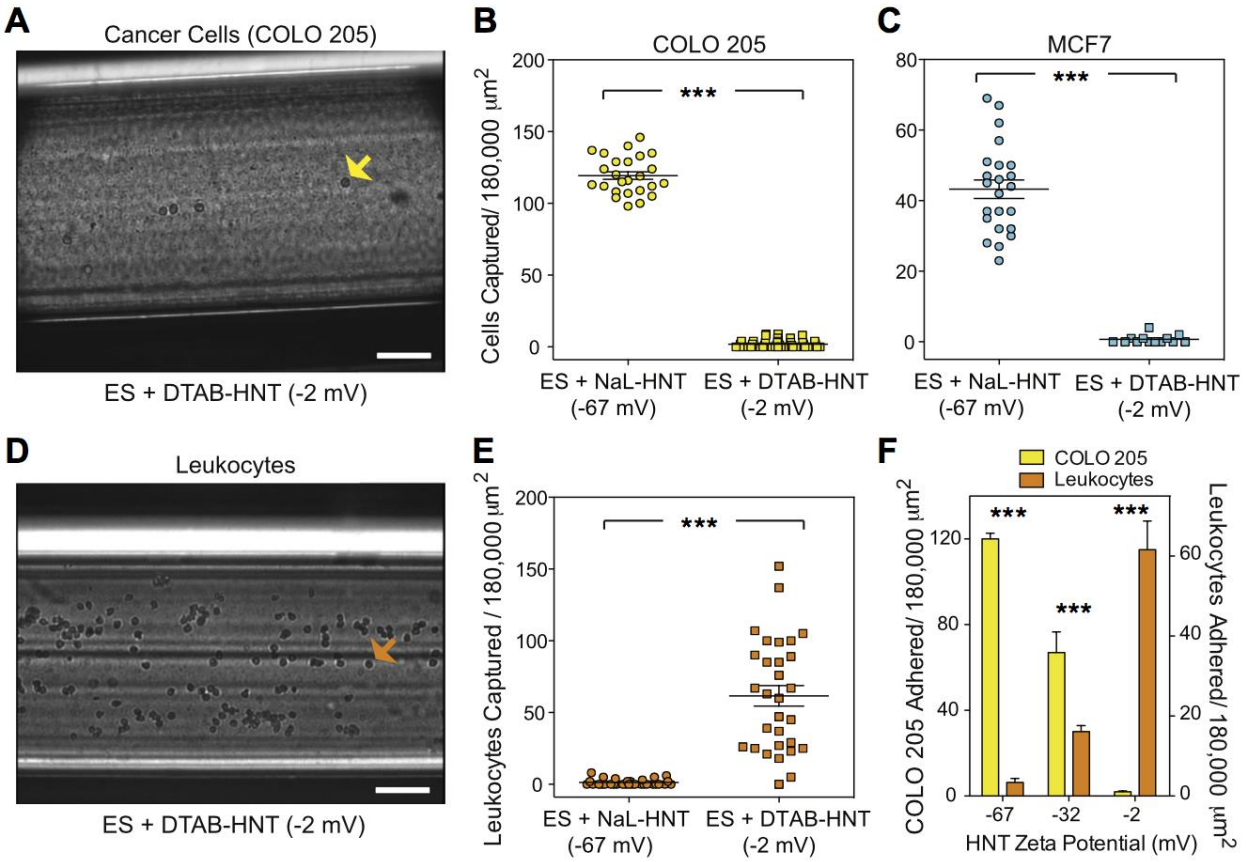

Fig. 4. HNT treatment with cationic surfactant reverses tumor cell and leukocyte capture on nanostructured biomaterial surfaces. Cancer cell and leukocyte capture on nano-structured surfaces under flow is dependent on HNT charge. (A) Negating HNT charge using DTAB surfactant abolishes cancer cell capture under flow. Yellow arrows denote adhered COLO 205 cells. Scale bar = 200 µm. (B, C) Number of captured COLO 205 (B) and MCF7 (C) cells per 180,000 µm^2. n = 20 or more image frames analyzed for each condition. Statistics calculated using a two-tailed unpaired t-test. ***P < 0.0001. (D) Negating HNT charge using DTAB surfactant restores leukocyte capture under flow. Orange arrows denote adhered leukocytes. Scale bar = 200 µm. (E) Number of captured leukocytes per 180,000 µm^2. Calculated values are mean ± SEM. N = 20 or more frames analyzed for captured cells for each condition. Statistics calculated using a two-tailed unpaired t-test. ***P < 0.0001. (F) Comparison of ES-mediated adhesion of leukocytes and COLO 205 cells per 180,000 µm^2 as a function of HNT zeta potential. Error bars denote standard error of the mean. Statistics were calculated using a two-tailed unpaired t-test. n = 30 or more image frames analyzed. ***P < 0.0001. (For interpretation of the references to color in this figure legend, the reader is referred to the web version of this article.)

physiological flow rates (flow rate = 0.04 mL/min, WSS = 2.5 dyn/cm^2) over surfaces consisting of ES + DTAB-HNT, it was evident that cancer cells interacted minimally with surfaces of diminished charge (Fig. 4A). The number of colon and breast cancer cells captured on DTAB-

HNT surfaces of minimal charge was reduced by >99% and >97%, respectively, compared to NaL-HNT surfaces of higher negative charge (Fig. 4B, C). Leukocyte adhesion under flow, absent on HNT surfaces of higher negative charge, was enhanced on ES + DTAB-HNT of diminished charge (Fig. 4D). Dampening of negative HNT charge increased the capture of free-flowing leukocytes by 60-fold, compared to ES + NaL-HNT surfaces of higher negative charge (Fig. 4E). Plotting the number of adherent cancer cells and leukocytes as a function of HNT zeta potential shows that HNT of higher negative charge can enhance cancer cell adhesion while minimizing leukocyte adhesion, and this adhesion response can be reversed by reducing the negative charge of HNT (Fig. 4F). Taken together, these results suggest that differential ES-mediated adhesion of cancer cells and leukocytes is dependent on surfactant functionalization and charge alteration of HNT.

To assess if HNT charge can directly mediate cell interactions, the effects of surfaces consisting of charged HNT, both in the presence and absence of ES, on cancer cell firm adhesion were examined. Few COLO 205 cancer cells firmly adhered to untreated HNT in the absence of ES (Fig. 5A), while the addition of ES allowed for successful recruitment and firm adhesion of cancer cells. Interestingly, surfaces consisting of highly negatively charged NaL-HNT alone, without ES immobilization, induced a significant in- crease in COLO 205 firm adhesion, compared to untreated HNT with immobilized ES. ES immobilization on NaL-HNT significantly increased COLO 205 cell firm adhesion, indicating that ES remains functional on NaL-HNT surfaces. However, given that ES only increased firm adhesion to NaL-HNT by ~15% compared

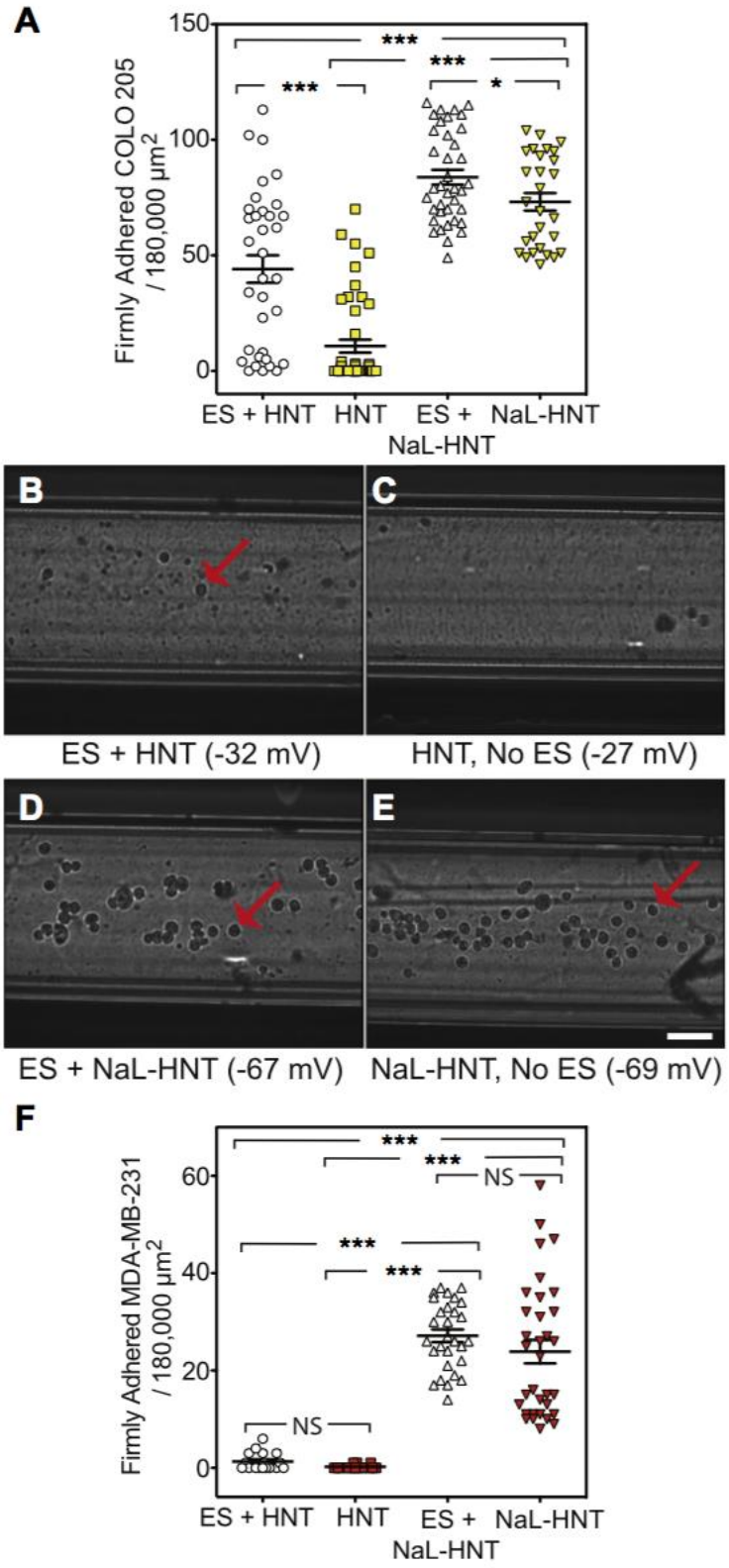

Fig. 5. NaL-HNT surfaces capture tumor cells in the absence of ES. (A) Firm adhesion of colorectal adenocarcinoma COLO 205 cells per 180,000 µm^2 to HNT and NaL-HNT in the presence and absence of the E-selectin (ES) adhesion receptor. Statistics were calculated

using a one-way ANOVA with Tukey post test. ***P < 0.0001. *P < 0.01. (B-E) Comparison of triple-negative breast cancer MDA-MB-231 cell capture on HNT sur- faces under flow, in presence and absence of ES adhesion proteins. Red arrows denote adhered MDA-MB-231 cells. Scale bar = 100 μm. (F) Captured MDA-MB-231 cells per 180,000 μm^2 to HNT surfaces in the presence and absence of the ES adhesion protein. Statistics calculated using a one-way ANOVA with Tukey post test. ***P < 0.0001. NS: not significant. (For interpretation of the references to color in this figure legend, the reader is referred to the web version of this article).

to NaL-HNT alone, it appears that surfactant immobilization plays a role in recruitment of tumor cells from flow. These results indicate that HNT charge affects the adhesion of COLO 205 cancer cells to surfaces consisting of negatively charged NaL-HNT.

In an effort to exploit adhesion of tumor cells in the absence of specific adhesion ligands, the adhesion of the metastatic MDA-MB- 231 breast cancer cell line to HNT-coated surfaces was examined. The MDA-MB-231 cell line is known as a "triple-negative" breast cancer (TNBC) cell type. Due to its lack of estrogen receptor, progesterone receptor, and human epidermal growth factor receptor 2 (HER2) expression, limited progress has been made in terms of therapeutic regimens for TNBC, and patients with the disease typically have the worst outcomes [47]. Additionally, MDA-MB-231 cancer cells have little to no ES ligand expression under normal culture conditions, and have been shown to engage in little to no interaction with ES and endothelial cells under flow [48,49]. Similar results were obtained in this study, as minimal MDA-MB-231 cells were found to adhesively interact with ES on HNT-coated surfaces, along with surfaces coated with untreated HNT alone (Fig. 5B, C, F). However, negatively charged NaL-HNT greatly enhanced the recruitment of MDA-MB-231 cells to the surface, both in the presence and absence of ES (Fig. 5D-F). NaL-HNT induced significant increases in the number of MDA-MB-231 cells captured from flow regardless of adhesion protein immobilization (Fig. 5F). These results suggest that NaL-HNT surfaces can be utilized to capture CTCs regardless of adhesion receptor expression. While immobilization of the ES adhesion receptor can enhance the

capture of cancer cells that express ES ligands, negatively charged NaL-HNT can be utilized to capture CTCs that do not express typical biomarkers or adhesion receptors.

1.5 Discussion

As cells approach a charged surface, the cell membrane can be either deformed toward the surface or away from it, depending on the charges present [50]. For cells expressing ES ligands, membrane deformation near charged surfaces could affect the number of cell ligands interacting with ES, and thus affect capture under flow conditions. Leukocytes have previously been reported to possess a negatively charged membrane potential [51]. Through coulombic interactions, leukocytes can be recruited to DTAB-HNT surfaces thereby enhancing ES ligation, while NaL-HNT repels leukocytes from approaching within a reactive distance to ES (Fig. 3F). Thus, it is logical that leukocytes with a high negative charge can be pre- vented from interacting with adhesion receptors on surfaces con- sisting of negatively charged HNT. What remains to be seen is how CTC capture is enhanced on surfaces consisting of HNT of high negative charge. Few studies have examined the zeta potential of cancer cells, and have generally found that zeta potential is less negative than that of leukocytes [52,53]. The answer to enhanced cancer cell capture on NaL-HNT could lie in the CTC glycocalyx, a gel-like layer of biologically inert macromolecules on the CTC surface that can extend as far as 500 nm from the CTC surface [54]. In particular, the synthesis of glycocalyx components can be impaired during malignant transformation, causing cancer cells to greatly over- express the glycocalyx component hyaluronan on their surface [55,56]. Additionally, leukocytes do not present a similar thick glycocalyx on surface. Thus, it is possible that components of the glycocalyx interact with NaL-HNT via electrostatic interactions, or potentially act as an adhesion ligand to the NaL surfactant. Future studies evaluating the surface charge of CTCs, and the effect of glycocalyx coatings could

shed further light on the mechanisms contributing to enhanced cancer cell adhesion to charged nanostructures.

1.6 Conclusion

The present study demonstrates, for the first time, that simple surfactant functionalization can induce a robust, differential adhesion response of tumor cells and blood cells on nanotube-coated surfaces. Surfaces consisting of differentially charged HNT can be fabricated without significant alteration in nanostructure. Functionalization of HNT with NaL was utilized to enhance the negative charge of HNT, which resulted in a significant increase in ES-mediated cancer cell adhesion while simultaneously repelling leukocyte adhesion. In the absence of ES, NaL-HNT surfaces suc- cessfully captured metastatic cells that do not express the adhesion receptor. Conversely, diminishing HNT charge with DTAB reversed the response, abolishing cancer cell adhesion while promoting leukocyte adhesion to ES. This straightforward method to functionalize HNT with surfactants not only shows that capture of tumor cells and blood cells is dependent on HNT charge, but also provides a unique platform to isolate CTCs, from patient blood for the development of personalized medicine regimens.

1.7 Acknowledgements

The authors gratefully acknowledge Jeff Mattison for work with blood sample collection and donor recruitment. The work described was supported by the Cornell Center on the Microenvironment and Metastasis through Award Number U54CA143876 from the National Cancer Institute. The content is solely the responsibility of the authors and does not necessarily represent the official views of the National Cancer Institute or the National Institutes of Health.

1.8 References

[1] Chaffer CL, Weinberg RA. A Perspective on Cancer Cell Metastasis. Science. 2011;331:1559–64. [PubMed]

[2] Chang YS, di Tomaso E, McDonald DM, Jones R, Jain RK, Munn LL. Mosaic blood vessels in tumors: frequency of cancer cells in contact with flowing blood. Proc Natl Acad Sci USA. 2000;97:14608–13. [PMC free article] [PubMed]

[3] Butler TP, Gullino PM. Quantitation of cell shedding into efferent blood of mammary adenocarcinoma. Cancer Research. 1975;35:512–6. [PubMed]

[4] Riethdorf S, Wikman H, Pantel K. Review: Biological relevance of disseminated tumor cells in cancer patients. International Journal of Cancer. 2008;123:1991–2006. [PubMed]

[5] Maheswaran S, Haber DA. Circulating tumor cells: a window into cancer biology and metastasis. Current Opinion in Genetics & Development. 2010;20:96–9. [PMC free article] [PubMed]

[6] Mitchell MJ, King MR. Fluid shear stress sensitizes cancer cells to receptor-mediated apoptosis via trimeric death receptors. New Journal of Physics. 2013;15:015008. [PMC free article] [PubMed]

[7] Mitchell MJ, King MR. Computational and experimental models of cancer cell response to fluid shear stress. Frontiers in Oncology. 2013;3:1–11. [PMC free article] [PubMed]

[8] Coussens LM, Werb Z. Inflammation and cancer. Nature. 2002;420:860–7. [PMC free article] [PubMed]

[9] Lawrence MB, Springer TA. Neutrophils roll on E-selectin. The Journal of Immunology. 1993;151:6339–46. [PubMed]

[10] McDonald B, Spicer J, Giannais B, Fallavollita L, Brodt P, Ferri L. Systemic inflammation increases cancer cell adhesion to hepatic sinusoids by neutrophil mediated mechanisms. International Journal of Cancer. 2009;125:1298–305. [PubMed]

[11] van Ginhoven TM, van den Berg JW, Dik WA, Ijzermans JNM, de Bruin RWF. Preoperative dietary restriction reduces hepatic tumor load by reduced E-selectin-mediated adhesion in mice. J Surg Oncol. 2010;102:348–53. [PubMed]

[12] Gassmann P, Kang ML, Mees ST, Haier J. In vivo tumor cell adhesion in the pulmonary microvasculature is exclusively mediated by tumor cell--endothelial cell interaction. BMC Cancer. 2010;10:177. [PMC free article] [PubMed]

[13] Yin X, Rana K, Ponmudi V, King MR. Knockdown of fucosyltransferase III disrupts the adhesion of circulating cancer cells to E-selectin without affecting hematopoietic cell adhesion. Carbohydrate Research. 2010;345:2334–42. [PMC free article] [PubMed]

[14] Rahn JJ, Chow JW, Home GJ, Mah BK, Emerman JT, Hoffman P, et al. MUC1 mediates transendothelial migration in vitro by ligating endothelial cell ICAM-1. Clinical & Experimental Metastasis. 2005;22:475–83. [PubMed]

[15] Mitchell MJ, Wayne E, Rana K, Schaffer CB, King MR. TRAIL-coated leukocytes that kill cancer cells in the circulation. Proc Natl Acad Sci USA. 2014;111:930–5. [PMC free article] [PubMed]

[16] Mitchell MJ, King MR. Leukocytes as carriers for targeted cancer drug delivery. Expert Opin Drug Deliv. 2014:1–18.

[17] Mitchell MJ, Castellanos CA, King MR. Nanostructured Surfaces to Target and Kill Circulating Tumor Cells While Repelling Leukocytes. Journal of Nanomaterials. 2012;2012:1–10. [PMC free article] [PubMed]

[18] Mitchell MJ, King MR. Unnatural killer cells to preventbloodborne metastasis: inspiration frombiology and engineering. Expert Rev Anticancer Ther. 2014;14:641–4. [PubMed]

[19] Hughes AD, Marshall JR, Keller E, Powderly JD, Greene BT, King MR. Differential drug responses of circulating tumor cells within patient blood. Cancer Letters. 2013 [PMC free article] [PubMed]

[20] Luo X, Mitra D, Sullivan RJ, Wittner BS, Kimura AM, Pan S, et al. Isolation and Molecular Characterization of Circulating Melanoma Cells. Cell Rep. 2014 [PMC free article] [PubMed]

[21] Greene BT, Hughes AD, King MR. Circulating Tumor Cells: The Substrate of Personalized Medicine? Frontiers in Oncology. 2012;2:1–6. [PMC free article] [PubMed]

[22] Allard WJ, Matera J, Miller MC, Repollet M, Connelly MC, Rao C, et al. Tumor cells circulate in the peripheral blood of all major carcinomas but not in healthy subjects or patients with nonmalignant diseases. Clin Cancer Res. 2004;10:6897–904. [PubMed]

[23] Yu M, Stott S, Toner M, Maheswaran S, Haber DA. Circulating tumor cells: approaches to isolation and characterization. The Journal of Cell Biology. 2011;192:373–82. [PMC free article] [PubMed]

[24] Miller MC, Doyle GV, Terstappen LWMM. Significance of Circulating Tumor Cells Detected by the CellSearch System in Patients with Metastatic Breast Colorectal and Prostate Cancer. J Oncol. 2010;2010:617421. [PMC free article] [PubMed]

[25] Nagrath S, Sequist LV, Maheswaran S, Bell DW, Irimia D, Ulkus L, et al. Isolation of rare circulating tumour cells in cancer patients by microchip technology. Nature. 2007;450:1235–9. [PMC free article] [PubMed]

[26] Hughes AD, Mattison J, Western LT, Powderly JD, Greene BT, King MR. Microtube Device for Selectin-Mediated Capture of Viable Circulating Tumor Cells from Blood. Clinical Chemistry. 2012;58:846–53. [PubMed]

[27] Bajpai S, Mitchell MJ, King MR, Reinhart-King CA. A microfluidic device to select for cells based on chemotactic phenotype. Technology. 2014;02:101–5. [PMC free article] [PubMed]

[28] Mitchell MJ, Chen CS, Ponmudi V, Hughes AD, King MR. E-selectin liposomal and nanotube-targeted delivery of doxorubicin to circulating tumor cells. Journal of Controlled Release. 2012;160:609–17. [PMC free article] [PubMed]

[29] Liu M, Guo B, Du M, Cai X, Jia D. Properties of halloysite nanotube-epoxy resin hybrids and the interfacial reactions in the systems. Nanotechnology. 2007;18:455703.

[30] Abdullayev E, Joshi A, Wei W, Zhao Y, Lvov Y. Enlargement of halloysite clay nanotube lumen by selective etching of aluminum oxide. ACS Nano. 2012;6:7216–26. [PubMed]

[31] Lvov YM, Shchukin DG, Möhwald H, Price RR. Halloysite clay nanotubes for controlled release of protective agents. ACS Nano. 2008;2:814–20. [PubMed]

[32] Veerabadran NG, Price RR, Lvov YM. Clay Nanotubes for Encapsulation and Sustained Release of Drugs. Nano. 2007;02:115–20.

[33] Cavallaro G, Lazzara G, Milioto S. Exploiting the Colloidal Stability and Solubilization Ability of Clay Nanotubes/Ionic Surfactant Hybrid Nanomaterials. J Phys Chem C. 2012;116:21932–8.

[34] Hughes AD, King MR. Use of Naturally Occurring Halloysite Nanotubes for Enhanced Capture of Flowing Cells. Langmuir. 2010;26:12155–64. [PubMed]

[35] Mitchell MJ, King MR. Shear-Induced Resistance to Neutrophil Activation via the Formyl Peptide Receptor. Biophysical Journal. 2012;102:1804–14. [PMC free article] [PubMed]

[36] Mitchell MJ, Lin KS, King MR. Fluid Shear Stress Increases Neutrophil Activation via Platelet-Activating Factor. Biophysical Journal. 2014;106:2243–53. [PMC free article] [PubMed]

[37] Horcas I, Fernández R, Gómez-Rodríguez JM, Colchero J, Gómez-Herrero J, Baro AM. WSXM: a software for scanning probe microscopy and a tool for nanotechnology. Rev Sci Instrum. 2007;78:013705. [PubMed]

[38] Silberberg MS. Chemistry: The molecular nature of matter and change. 5. McGraw Hill; 2008.

[39] Chen W, Weng S, Zhang F, Allen S, Li X, Bao L, et al. Nanoroughened Surfaces for Efficient Capture of Circulating Tumor Cells without Using Capture Antibodies. ACS Nano. 2013;7:566–75. [PMC free article] [PubMed]

[40] Ball C, King M. Role of c-Abl in L-selectin shedding from the neutrophil surface. Blood Cells, Molecules, and Diseases. 2011;46:246–51. [PMC free article] [PubMed]

[41] Cao TM, Mitchell MJ, Liesveld J, King MR. Stem Cell Enrichment with Selectin Receptors: Mimicking the pH Environment of Trauma. Sensors. 2013;13:12516–26. [PMC free article] [PubMed]

[42] Kim MB, Sarelius IH. Distributions of Wall Shear Stress in Venular Convergences of Mouse Cremaster Muscle. Microcirculation. 2003;10:167–78. [PubMed]

[43] Myung JH, Gajjar KA, Pearson RM, Launiere CA, Eddington DT, Hong S. Direct measurements on CD24-mediated rolling of human breast cancer MCF-7 cells on E-selectin. Analytical Chemistry. 2011;83:1078–83. [PMC free article] [PubMed]

[44] Shafie SM, Liotta LA. Formation of metastasis by human breast carcinoma cells (MCF-7) in nude mice. Cancer Letters. 1980;11:81–7. [PubMed]

[45] Mattila MMT, Ruohola JK, Karpanen T, Jackson DG, Alitalo K, Härkönen PL. VEGF-C induced lymphangiogenesis is associated with lymph node metastasis in orthotopic MCF-7 tumors. Int J Cancer. 2002;98:946–51. [PubMed]

[46] Kawada K, Hosogi H, Sonoshita M, Sakashita H, Manabe T, Shimahara Y, et al. Chemokine receptor CXCR3 promotes colon cancer metastasis to lymph nodes. Oncogene. 2007;26:4679–88. [PubMed]

[47] Tate CR, Rhodes LV, Segar HC, Driver JL. Targeting triple-negative breast cancer cells with the histone deacetylase inhibitor panobinostat. Breast Cancer Research. 2012;14:R79. [PMC free article] [PubMed]

[48] Julien S, Ivetić A, Grigoriadis A, QiZe D, Burford B, Sproviero D, et al. Selectin Ligand Sialyl-Lewis x Antigen Drives Metastasis of Hormone-Dependent Breast Cancers. Cancer Research. 2011;71:7683–93. [PubMed]

[49] Evani SJ, Prabhu RG, Gnanaruban V, Finol EA, Ramasubramanian AK. Monocytes mediate metastatic breast tumor cell adhesion to endothelium under flow. The FASEB Journal. 2013;27:3017–29. [PMC free article] [PubMed]

[50] Vorobyov I, Bekker B, Allen TW. Electrostatics of deformable lipid membranes. Biophysical Journal. 2010;98:2904–13. [PMC free article] [PubMed]

[51] Parodi A, Quattrocchi N, van de Ven AL, Chiappini C, Evangelopoulos M, Martinez JO, et al. Synthetic nanoparticles functionalized with biomimetic leukocyte membranes possess cell-like functions. Nature Nanotechnology. 2012;8:61–8. [PMC free article] [PubMed]

[52] Zhang Y, Yang M, Park JH, Singelyn J, Ma H, Sailor MJ, et al. A surface-charge study on cellular-uptake behavior of F3-peptide-conjugated iron oxide nanoparticles. Small. 2009;5:1990–6. [PMC free article] [PubMed]

[53] Zhang Y, Yang M, Portney NG, Cui D, Budak G, Ozbay E, et al. Zeta potential: a surface electrical characteristic to probe the interaction of nanoparticles with normal and cancer human breast epithelial cells. Biomed Microdevices. 2008;10:321–8. [PubMed]

[54] Mitchell MJ, King MR. Theme: Physical Biology in Cancer. 3. The role of cell glycocalyx in vascular transport of circulating tumor cells. AJP: Cell Physiology. 2014;306:C89–C97. [PMC free article] [PubMed]

[55] Hopwood JJ, Dorfman A. Glycosaminoglycan synthesis by cultured human skin fibroblasts after transformation with simian virus 40. Journal of Biological Chemistry. 1977;252:4777–85. [PubMed]

[56] Itano N, Kimata K. Altered hyaluronan biosynthesis in cancer progression. Seminars in Cancer Biology. 2008;18:268–74. [PubMed]

Chapter 2

Exploiting Serum Interactions with Cationic Biomaterials Enables Label-Free Circulating Tumor Cell Isolation

2.1 Abstract

Mounting evidence has shown that, in biological fluids, proteins adsorbed to the surfaces of nanomaterials that are known as protein corona can critically affect the interactions of the nanomaterials with living cells. Little is known, however, about how abundant free proteins in biological systems can influence such physical interactions. By using a model systems−microscale flow device, we demonstrate for the first time that free serum proteins can greatly modulate electric charge interactions between materials and cells (white blood cells and cancer cells) through enhanced fluid dielectric. We found that such an effect was independent of protein fouling. We show further that living cells (cancer cells and white blood cells) with surface charges ranging from -8mV through -22mV present significantly varying interactions with positively charged surfaces only in the presence of free proteins. Moreover, when microparticles with surface charge matched to that of cells interact with positively charged materials, the observed difference is found to depend solely on the surface charge of cells irrespective of the origin of those cells. Lastly, we observed that the level of heparan sulfate proteoglycans on a cell surface correlates with cell charge and thus contributes to differential interactions between cells and positively charged surfaces. Insofar as many gene delivery and cell isolation platforms rely on electrical interactions between living cells and materials, our study could reveal a new determinant of efficient adhesion and targeting in the context of a biological-fluid environment.[2]

[2] The content of this chapter was presented at a conference:

Carlos A. Castellanos*, Michael J. Mitchell*, Michael R. King, "Exploiting Serum Interactions with Cationic Biomaterials Enables Label-Free Circulating Tumor Cell Isolation"

***Authors contributed equally to this work.**

C.A.C, M.J.M., and M.R.K. conceived of research; C.A.C., M.J.M., and M.R.K. designed research; C.A.C. and M.J.M. performed research; M.J.M. and C.A.C. analyzed data; M.J.M., C.A.C., and M.R.K. wrote the paper.

2.2 Introduction

By definition biomaterials interface with biological systems, including bodily fluids and a variety of cell types [1-3]. They have gained overwhelming popularity due to the wide range of applications for which they are suitable in diagnostic devices [4-5], implantations, and drug delivery [6-10]. Meanwhile, they remain under intensive study, as the ultimate goal of biomaterials is biocompatibility in material–host interaction, cytotoxicity, degradation, and so on [11-12]. For certain medical applications, biomaterials are designed to support cell adhesion in stem cell implantation or the introduction of large molecules into cells in the delivery of nucleic acids or antigens [13-16]. Current schemes for facilitating material–cell interaction generally fall into two categories. The first type involves using bio-specific molecules to achieve targeted specificity including antibodies, peptides, and aptamers [17-19]. In the other scheme, electrostatic interactions, especially those with cationic materials, have been widely used in regenerative medicine for the following reasons: (1) They are relatively inexpensive compared with biomolecules, particularly when the materials need to be scaled up; (2) nearly all types of cells (including bacteria and mammalian cells) are negatively charged on the surface so that cationic materials can potentially target universal cell types when specificity is unnecessary [20-23]; and (3) their ability to be easily modified makes them attractive for many biological applications [24]. As a result, there has been a vast amount of research focusing on designing novel natural or synthetic cationic polymers with specific biological functionality. For example, poly (L-lysine) (PLL) and polyethylenimine (PEI) are considered efficient nucleic acid-condensing agents in non-viral gene delivery systems [25].

However, owing to surface charge and structure, biomaterials—including cationic polymers—are capable of adsorbing biomolecules upon contact with biological systems [26-27].

In particular, over the past few years several investigations have shown that proteins can bind to the surface of nanomaterials commonly known as protein corona in the context of biological fluids such as serum [28]. Importantly, the formation of such a protein layer can alter the biological identity of the nanomaterials and therefore affect biomedical applications. Moreover, cationic materials are found to have elevated adsorption of proteins compared with neutral polymers [29-30]. Despite extensive studies on immobilized protein corona, no study has been carried out to examine how free proteins in biological fluid can modulate electric charge interactions between biomaterials and cells in light of broad interest in utilizing cationic materials for biomedical applications.

Since cationic biomaterials commonly interface with cells in the presence of biological fluids containing a large amount of proteins, we reasoned that such free proteins can modulate fluid dielectric and thereby affect interactions between charged objects, as suggested by Coulomb's Law. We measured the surface charge of cells of varying origins and found that the cells present a broad range of negative charge, from -8mV to -22mV. Moreover, the cells interacted with cationic materials differently (from no interaction to moderate or strong adhesion) depending on their specific surface charge in the presence of buffered saline containing albumin, the most abundant protein in the serum.

2.3 Materials and Methods

2.3.1 Cell Culture

Human breast adenocarcinoma cell line MDA-MB-231 (ATCC #HTB-26), lung carcinoma cell line A549 (ATCC #CCL-185) and colorectal carcinoma cell line HCT-116 (ATCC #CCL-247) were purchased from American Type Culture Collection (ATCC; Manassas, VA, USA). MDA-MB-231 cells were grown in DMEM supplemented with 10% fetal bovine

serum (FBS) and 1% PenStrep (PS), all purchased from Invitrogen (Grand Island, NY, USA). A549 and HCT-116 cells were cultured in RPMI 1640 supplemented with 10% FBS, and 1% PenStrep, all purchased from Invitrogen. All cell lines were incubated under humidified conditions at 37° C and 5% CO2, and not allowed to exceed 90% confluence. In preparation for capture assays, cancer cells were removed from culture via treatment with enzyme free cell dissociation buffer (ThermoFisher) for 30 min prior to handling. Cells were washed in PBS, and resuspended at a concentration of 5.0 x 10^5 cells/mL in PBS flow buffer supplemented with 0 - 1% human serum albumin, 2 mM Ca2+, and 10 mM HEPES (Invitrogen), buffered to pH 7.4.

2.3.2 Mononuclear Leukocyte Isolation

Human leukocytes were isolated as described previously. Briefly, human peripheral blood was collected from healthy blood donors via venipuncture after informed consent and stored in heparin containing tubes (BD Biosciences, San Jose, CA, USA). Blood was carefully layered over Ficoll-Paque (GE Healthcare Life Sciences) and separated via centrifugation using a Marathon 8K centrifuge (Fisher Scientific, Pittsburgh, PA, USA) at 2400 rpm for 15 min. Mononuclear leukoctyes were extracted and washed in cation-free HBSS, and excess red blood cells were lysed hypotonically. Prior to capture assays, leukocytes were resuspended in PBS flow buffer supplemented with 0-1% human serum albumin (HSA), 2mM Ca2+, and 10 mM HEPES (Invitrogen), buffered to pH 7.4.

2.3.3 Fabrication of Polymer-Coated Surfaces

Microrenathane (MRE) tubing (Braintree Scientific, Braintree, MA, USA) of inner diameter 300 μm was cut to 55 cm in length and fastened onto the stage of an Olympus IX-71 inverted microscope (Olympus, Center Valley, PA, USA). To functionalize the inner MRE surface with cationic polymer, microtubes were washed thoroughly with distilled water, followed

by incubation with aqueous 0.025 – 0.1% poly-L-lysine, polyethyleneimine, or poly(allyl)amine for 30 min. Microtubes were then washed thoroughly with distilled water to remove nonadsorbed polymer, and used immediately for cell capture assays.

2.3.4 Cell Capture Assays

Cell suspensions were perfused through microtubes using a motorized syringe pump (KDS 230; IITC Life Science, Woodland Hills, CA, USA) and monitored via an inverted microscope linked to a Hitachi CCD KP-M1AN camera (Hitachi, Japan) and a Sony DVD Recorder DVO-1000MD (Sony Electronics Inc., San Diego, California, USA). All cells and particles were perfused at 0.008 mL/min (wall shear stress of 0.5 dyn/cm2) for 10 min, and then 0.008 mL/min for another 10 min to remove un-adhered cells. The number of adhered cells was taken from up to 30 random video frames for each microtube. "Firmly adhered cells" denote cells that were captured from flow.

2.3.5 Cell Electric Charge Characterization

To evaluate the electric charge of cells, zeta potential (mV) of all cell samples treated and un-treated with *Bacteroides* Heparanase III (New England BioLabs Inc.) were measured by dynamic light scattering (DLS) using a Malvern Zetasizer Nano ZS (Malvern Instruments Ltd., Worcestershire, UK). To assess expression of heparan sulfate proteoglycans on cell surfaces, Anti-Heparan Sulfate Proteoglycan 2 antibody [A74] (ab23418) was added to cell suspension and adherent antibody determined using flow cytometry.

2.3.6 Fluid Dielectric Measurements

Fluid dielectric constant was measured using a Novocontrol Broadband Dielectric Spectrometer (Montabaur/ Germany) at 100 Hz frequency. Air was used to simulate vacuum

capacitance. Measured capacitance of water and aqueous albumin solutions used to determine dielectric constants by dividing measured values with the capacitance of air.

2.3.7 Immunofluorescence Preparation of CTCs Isolated from Cancer Patient Blood

Following processing with PLL-coated devices, captured cells were released from the microtube and plated onto 8 mm, #1.5 thickness coverslips (Electron Microscopy Services, Hatfields, PA, USA) coated with 1% Cell-Tak (Corning). Cells were fixed with 2% formaldehyde in 50% Phem buffer (60 mM PIPES, 25 mM HEPES, 10 mM EGTA, 2 mM $MgCl_2$) and blocked overnight in 10% Normal Goat Serum (Jackson ImmunoResearch, PA, USA) and 6% Bovine Serum Albumin in DPBS (Corning). Cells were then processed for immunofluorescence labeling. The following antibodies were used: mouse monoclonal anti-CD45 directly conjugated with QDot 800 (Invitrogen, Carlsbad, CA), mouse monoclonal anti-EpCAM directly conjugated with Alexa Fluor 647 (Biolegend), mouse monoclonal anti-PSMA (J591) directly conjugated with fluorescein isothiocyanate (FITC, provided by Dr. Neil Bander, Weill Cornell Medical College, NY, USA). Cells were then permeabilized with 0.25% Triton X-100 (Sigma) and stained with mouse monoclonal anti pan-cytokeratin (Biolegend) directly conjugated with CF594 (Biotium). DNA was stained with 1 μg mL^{-1} 4’,6-diamidino-2-phenylindole (DAPI; Sigma). The cells were mounted using Mowiol.

2.3.8 CTC Identification and Downstream High Resolution Confocal Microscopy

Low resolution, multiplex tile scanning of the coverslips was performed using a 10x objective (Zeiss, Germany). Reconstructed tile scans of coverslips were subjected to an algorithm to identify putative CTCs based on size and shape, DAPI positivity, cytokeratin positivity, and CD45 negativity. Individual positions of CTCs are marked and rank-ordered by

descending CK staining intensity and subjected to high resolution imaging. Putative CTCs were imaged at high resolution with 20-50 individual z-slices at 0.24 um per z-plane recorded for each cell. Images were acquired using Yokogawa CSU-X1 confocal microscope with a 63x/1.4NA objective (Zeiss). Three-dimensional image reconstruction was performed and manually reviewed in order to eliminate false positive CTCs. CTCs were confirmed on basis of DAPI, cytokeratin, and CD45 staining. Only confirmed CTCs were included in final enumeration.

2.3.9 Statistical Analysis

Data sets were plotted and analyzed using Microsoft Excel (Microsoft, Redmond, WA, USA) and GraphPad Prism 5.0 (GraphPad software, San Diego, CA, USA). All results were reported as the mean +/- standard error of the mean (SEM) or standard deviation (SD) as indicated. Two-tailed paired and unpaired t-tests, and one-way ANOVA with Tukey post-tests were utilized for statistical analyses. *P*-values less than 0.05 were considered significant.

2.4 Results

2.4.1 Malignant Neoplasms Express Heparan Sulfate Proteoglycans

We are interested in exploiting differences in cell membrane electric phenotype to differentially capture cancer cells and blood cells under continuous flow conditions. Cancer cells express negatively charged heparan sulfate proteoglycans on their cell membranes; such proteoglycans are lacking on white blood cells (Figure 1a). The differential expression of proteoglycans results in differences in the electric charge of cells as measured by electrophoretic mobility, with cancer cells having higher negative electric charge than blood cells (Figure 1 b). Treating cells with heparanases to remove heparan sulfate proteoglycans diminishes the electric charge of cancer cells while that of white blood cells remains unchanged (Figure 1 b). Together these results demonstrate that cell surface proteoglycans contribute to differences in electric

charge between cancer cells and white blood cell types. Cancer cell expression of heparan sulfate proteoglycans results in these cells having elevated negative electric charge compared with white blood cells, which do not express heparan sulfate residues on their surfaces.

A

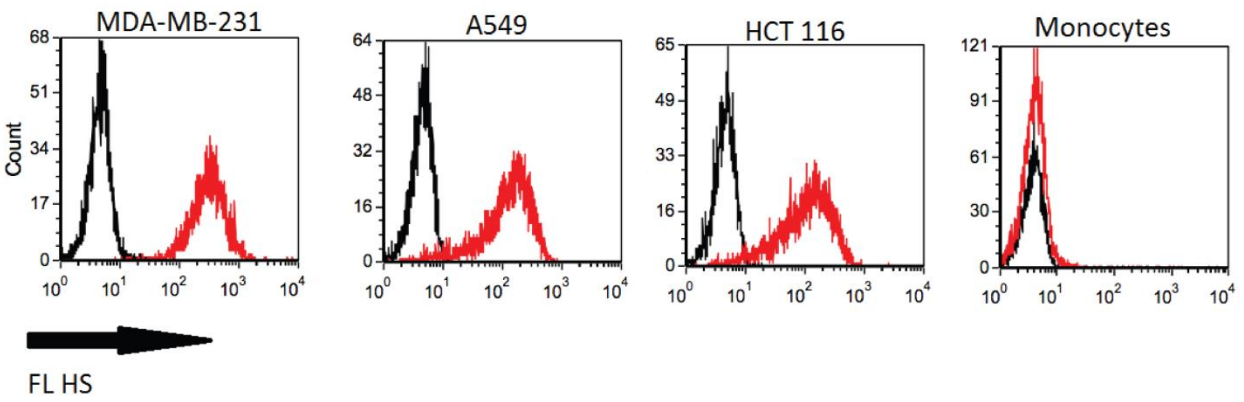

B

Cell Type	Zeta Potential (mV)	Zeta Potential (mV) HeparanaseIII Treated
MDA-MB 231	-14.9 ± 1.8	-9.4 ± 0.4
A549	-14.7 ± 1.9	-7.4 ± 0.4
HCT116	-13.0 ± 0.5	-9.8 ± 0.7
Monocytes	-10.6 ± 0.5	-10.3 ± 1.2

Figure 1: Characterization of cancer cell and white blood cell electric phenotype. (A) To assess expression of negatively charged heparan sulfate proteoglycans on cell surfaces, fluorescent anti-heparan sulfate antibody was added to cancer cells and mononuclear leukocytes for 45 minutes. Expression of fluorescent anti-heparan sulfate antibody on the surface of cancer cells and blood cells determined using flow cytometry. (B) Zeta potential measurements of cancer cells and white blood cells before and after treatment with heparanse III. Values are mean ± standard deviation (n = 3).

2.4.2 Cell Adhesion to Cationic Polymer Coated Microscale Flow Devices

To test the adhesive potential of cells to cationic polymer-coated surfaces, three polymers at varied concentrations were individually adsorbed to the inner lumen of microscale flow devices and each device was used to measure the adhesive potential of malignant and non-

malignant cells under flow (Figure 2A-B). Cells suspended in flow buffer containing 0.5% w/v serum albumin adhesively interacted with polymer-coated surfaces in a manner that depended on the concentration of cationic polymer adsorbed to the surfaces, with the greatest number of cancer and white blood cells firmly adhered on surfaces treated with 0.1% w/v cationic polymer (Figure 2 C – E). Surfaces coated with 0.025% w/v poly-L-lysine had the lowest number of white blood cells adhered while also showing elevated capture of the breast cancer cell line MDA-MB 231 (Figure 2 C). For this reason poly-L-lysine was chosen to study the effect fluid dielectric has on adhesive interactions between cells and charged surfaces.

2.4.3 Serum Albumins Modulate Fluid Dielectric and Adhesive Interactions Between Cells and Poly-L-Lysine Coated Surfaces Under Flow

Aqueous fluids have a high dielectric constant due to the polar nature of water molecules, which become ordered in the presence of electric fields [31]. Adding the protein human albumin to water increases the fluid's electric permittivity and thus its dielectric constant (Figure 3 A). The increased fluid dielectric could in turn affect how electrical charges interact according to the force equations that describe those interactions (e.g., Coulomb's law). To study the effect proteins have on cell adhesion to PLL-coated surfaces, we progressively suspended cells in buffers containing varying amounts of human serum albumin and flowed cells through PLL-coated microscale flow devices. Blood cells suspended in a protein-free buffer adhesively interacted with poly-L-lysine under continuous flow in a manner that depended on the concentration of polymer adsorbed to the surface of microscale flow devices, suggesting that surfaces coated with higher concentrations of PLL contained higher electric charge density, allowing cells to form more adhesive electrostatic interactions (Figure 3 C). Interestingly, the addition of 0.5% w/v serum albumin to white cell buffer solution decreased white cell adhesion to surfaces coated with 0.025% poly-L-lysine, but white cell adhesion increased as the

concentration of poly-lysine adsorbed onto surfaces increased (Figure 3 C). Increasing albumin concentration further to 1% w/v nearly abrogated firm adhesion of white blood cells to PLL-coated surfaces while maintaining cancer cell adhesion at levels similar to those observed in protein-free and 0.5% albumin buffer solutions (Figure 3B), indicating that adding proteins to a buffer solution effectively modulates the potential of cells to adhere to charged surfaces according to their electric phenotype (Figure 3 B - C).

Cancer cells expressing highly negative heparin sulfate proteoglycans showed increased electric charge compared with white blood cells (figure 1 B), and thus are able to form adhesive interactions with PLL-coated surfaces in higher dielectric media. Indeed, cleaving heparin sulfate proteoglycans from cancer cells reduced electric charge (Figure 1 C) and also reduced adhesion of these cells to PLL-coated surfaces (Supplementary figure 1). Polystyrene particles with electrical charge matched to that of cancer and blood cells used in this study were also observed to differentially interact with PLL-coated surfaces in protein-containing solutions (Supplementary figure 2).

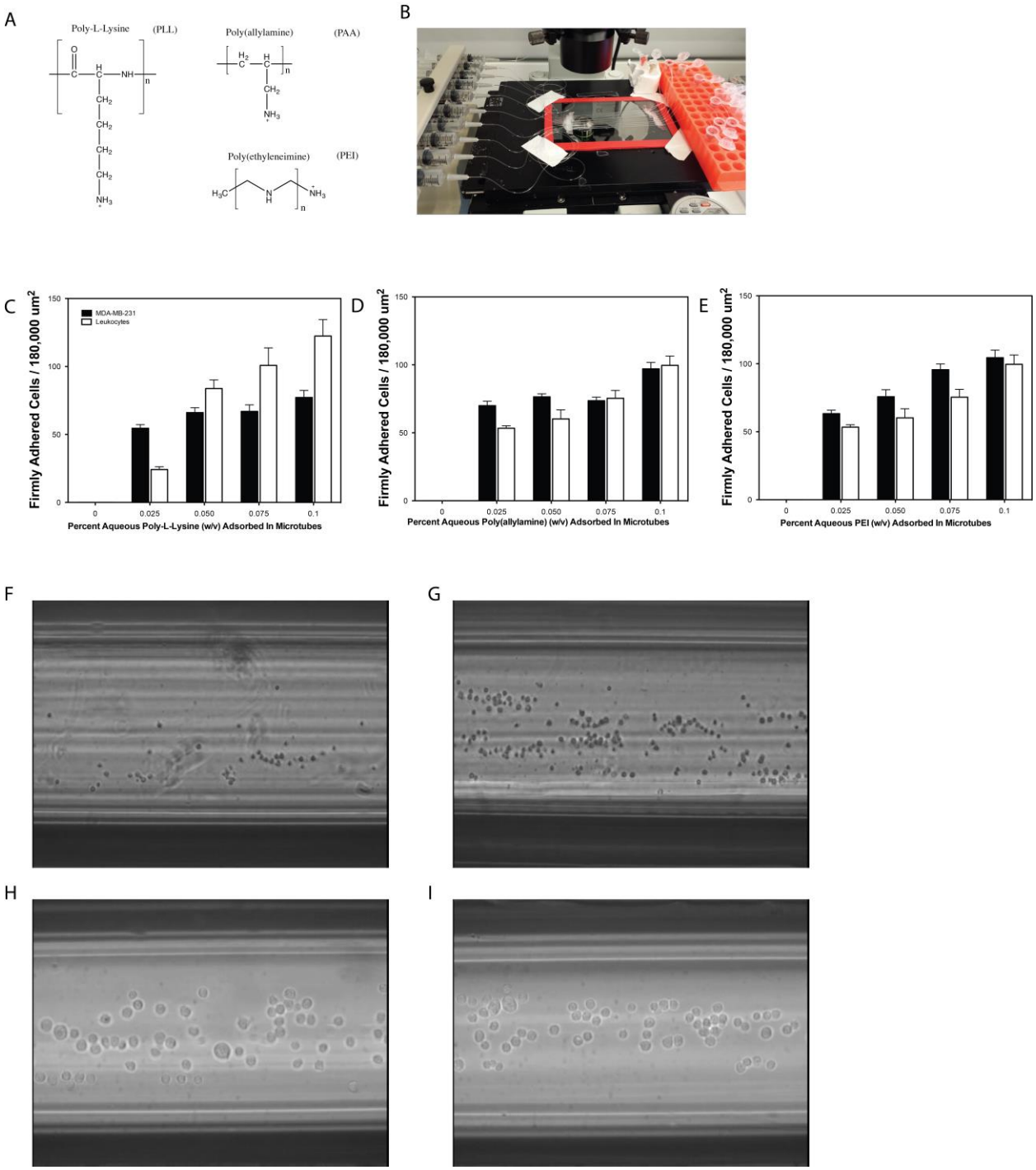

Figure 2: Cell adhesion to cationic polymer coated surfaces under continuous flow. (A) Atomic structure of cationic polymers Poly-L-Lysine (PLL), Poly(allylamine) (PAA), and Poly(ethyleneimine) (PEI) used for capturing cells on treated surfaces. (B) Photograph of microscale flow devices mounted onto the stage of microscope and attached to motorized syringe pump. (C – E) Number of firmly adhered MDA-MB-231 breast cancer cells (black bars) and mononuclear leukocytes (white bars) per 180,000 um^2 on surfaces coated with 200 uL of 0.025 - 0.1% (w/v) cationic polymer. Cancer cells (500,000 cells/mL) and white blood cells (1,000,000 cells/mL) were suspended in flow buffer containing 0.5% (w/v)

human serum albumin and flowed through devices at a flow rate of 0.008 mL/min (wall shear stress of 0.5 dyn/cm^2) for 10 minutes. Surfaces were then washed another ten minutes with same flow buffer to obtain number of firmly adhered cells. (F – G) Images of leukocytes captured on surfaces functionalized with 0.025% w/v PLL (F) or 0.1% w/v PLL (G). (H – I) Images of MDA-MB-231 breast cancer cells captured on surfaces functionalized with 0.025% w/v PLL (H) or 0.1% w/v PLL (I).

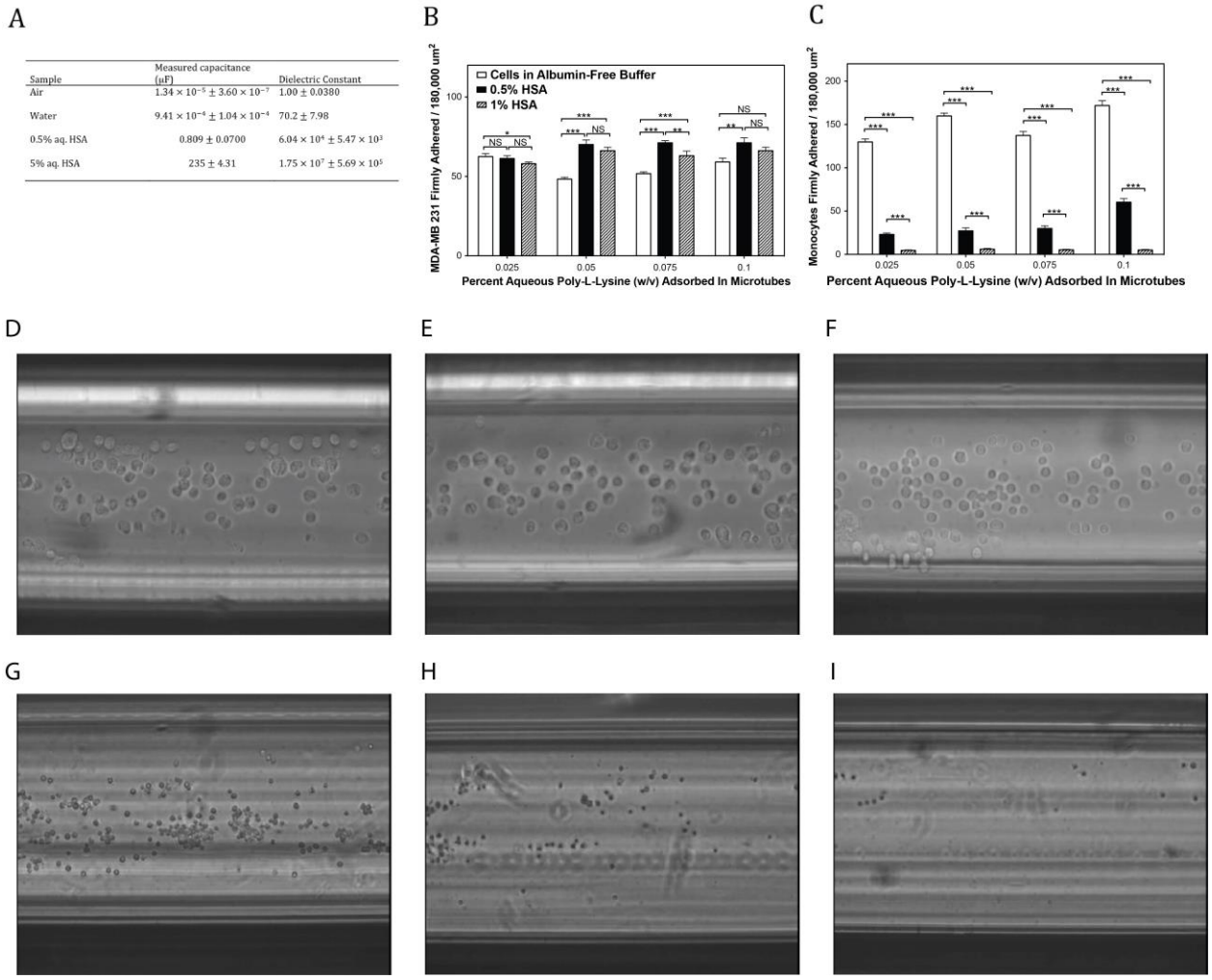

Figure 3: Human serum albumin modulates fluid dielectric and cellular adhesion to PLL-coated surfaces under continuous flow. (A) Measured capacitance of air, water, and aqueous human serum albumin at concentration of 0.5 and 5% (w/v) albumin. Capacitance values were used to calculate the dielectric constant by dividing by capacitance of air. Calculated values are mean ± standard deviation (n = 3). (B - C) Number of firmly adhered MDA-MB-231 breast cancer cells and mononuclear leukocytes per 180,000 um^2 on surfaces coated with 200 uL of 0.025 – 0.1% (w/v) PLL. Cancer cells (500,000 cells/mL) and white blood cells (1,000,000 cells/mL) were suspended in PBS flow buffer containing 0% (white bars), 0.5%(black bars), or 1%(striped bars) human serum albumin (HSA) and flowed through devices at a flow rate of 0.008 mL/min (wall shear stress of 0.5 dyn/cm^2) for 10 minutes. Surfaces were then washed for ten minutes with same flow buffer used for each condition tested to remove un-adhered cells. n = 20 or more frames analyzed for captured cells for each condition. Statistics were calculated using a one-way ANOVA with

Tukey post test. ***$P < 0.0001$, **$P < 0.001$, *$P < 0.01$, NS: not significant. (D – E) Images of MDA-MB-231 cancer cells captured on surfaces functionalized with 0.1% w/v PLL and cells suspended in PBS flow buffer supplemented with (D) 0%, (E) 0.5%, or (F) 1% w/v HSA. (G – I) Images of leukocytes captured on surfaces functionalized with 0.1% w/v PLL and cells suspended in PBS flow buffer supplemented with (G) 0%, (H) 0.5%, or (I) 1% w/v HSA.

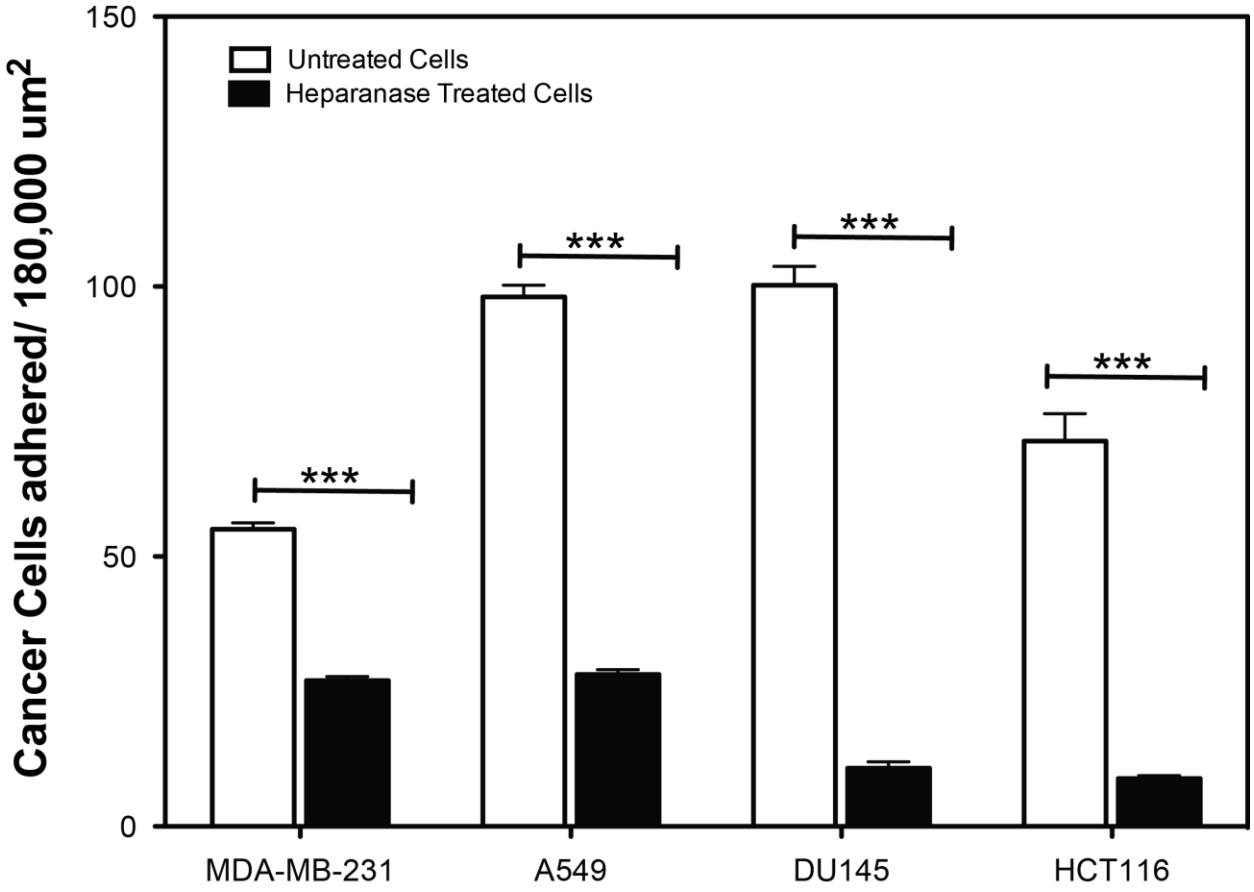

Supplementary Figure 1: Heparanase treatment reduces adhesion of cancer cells to PLL coated surfaces under flow conditions. Heparanase III treated and untreated cells were perfused through microscale flow devices at flow rate 0.008 mL/min (wall shear stress 0.5 dyn/cm^2) for 10 minutes. Unadhered cells were removed by perfusing flow buffer at the same rate for another ten minutes. n = 20 or more frames analyzed for captured cells for each condition. Statistics were calculated using a two-tailed unpaired t-test. ***$P < 0.0001$.

Altogether, these data show that negatively charged cell adhesion to cationic surfaces can be controlled by at least three variables: 1) the concentration of cationic polymer adsorbed on surfaces, which could correlate with the electric charge density of capture surfaces; 2) the electric charge of cell surfaces controlled by the expression of cell surface residues such as

heparan sulfate proteoglycans; and 3) the dielectric properties of the fluid modulated by the addition of albumin to the solution. These three variables can be tuned to affect cell adhesion to charged surfaces, providing scientists and clinicians with a new way of targeting rare cells of interest by controlling capture surface and fluid properties.

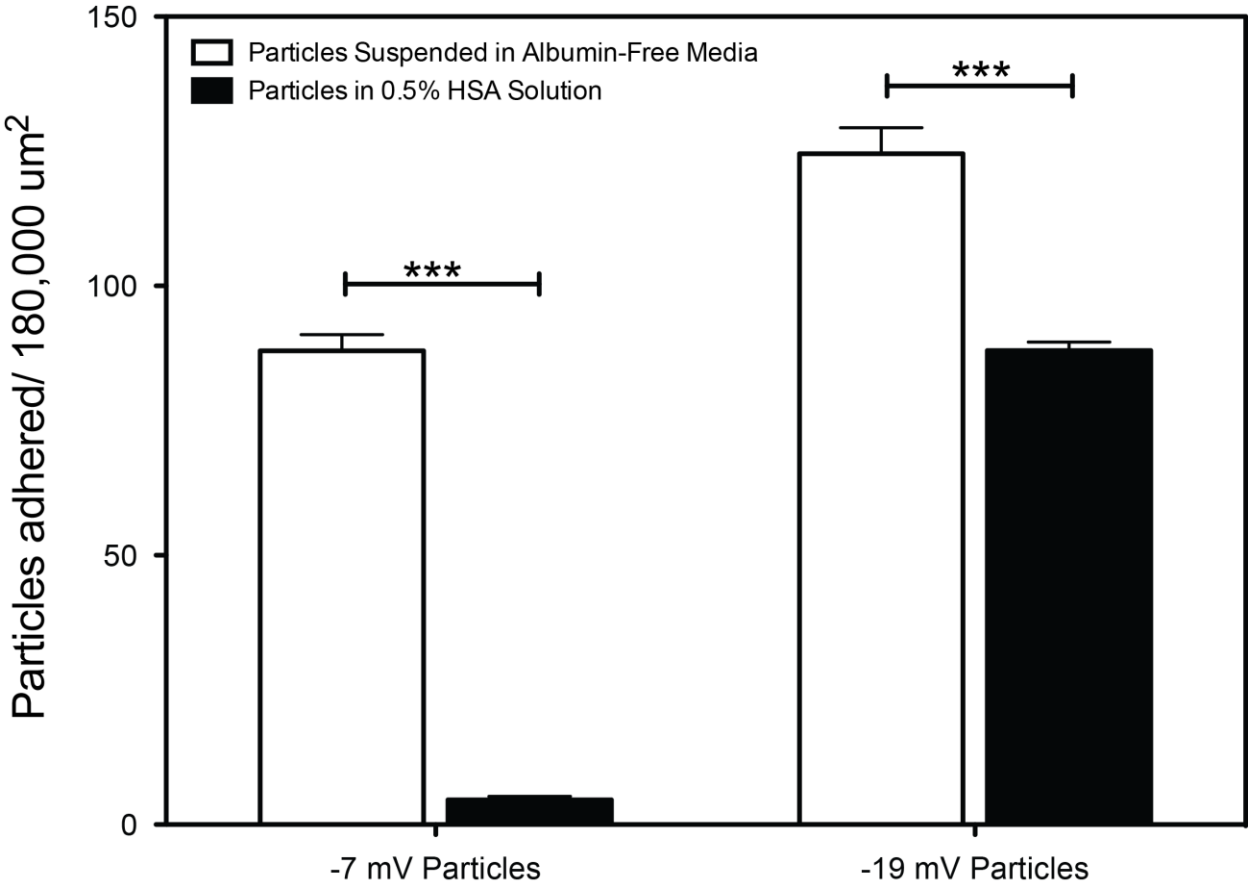

Supplementary Figure 2: Negatively charged polystyrene particles differentially adhere to PLL coated surfaces in protein-containing buffer solution. 10 um sized polystyrene particles (0.025% w/v) possessing measured zeta potentials of -7 and -19 mV were suspended in PBS buffer with or without 0.5% (w/v) human serum albumin. -19 mV particles were produced by incubating -7 mV stock particles in 1% polystyrene sulfonate solution for 1 hour and washing particles 3 times to obtain functionalized negatively charged particles. Particles were then flowed through PLL functionalized microscale flow devices containing 200 uL of 0.1% (w/v) PLL for 10 minutes at a flow rate of 0.008 mL/min (wall shear stress 0.5 dyn/cm^2). Unadhered particles were removed by perfusing flow buffer at the same rate for another ten minutes. n = 20 or more frames analyzed for captured cells for each condition. Statistics were calculated using a two-tailed unpaired t-test. ***P < 0.0001.

2.4.4 Isolation of CTCs from Blood of Metastatic Prostate Cancer Patients

Approximately 1 CTC is present for every one million leukocytes in a given patient blood sample, and CTCs and leukocytes both adhesively interact with cationic surfaces (Fig. 2C – E). However, enhancing fluid dielectric with albumin nearly abrogated firm adhesion of leukocytes to charged surfaces (Fig. 3C). For this reason, blood taken from patients diagnosed with late-stage prostate cancer was spun down to obtain a buffy coat layer, and subsequently suspended in buffer containing 1% HSA to minimize white cell fouling. The sample was then processed using microscale flow devices the inner lumen of which was functionalized with PLL to capture potential CTCs (Figure 4). Currently the state of the art for CTC detection utilizes monoclonal antibodies against transmembrane proteins such as epithelial cell adhesion molecules (EpCAM). Interestingly, some patients contained CTCs that were EpCAM+ and in the same blood sample CTCs that were $EpCAM^-$ (Figure 4B).

2.5 Discussion

An object in motion will continue in motion unless acted on by external force [32]. In our experiments we set cells in motion using a motorized syringe pump and observed changes in the state of the cells' motion as they transitioned from continuous flow to firm adhesion on charged surfaces. A change in motion is called acceleration. Whenever an object accelerates there must be a cause of that acceleration, and that cause is called the force:

$$F = ma$$

In the above equation 'F' is the net force, 'm' is the mass, and 'a' is the acceleration of the object. We commonly invoke four fundamental forces to describe interactions between objects and materials. The most familiar force is gravitation, which is responsible for apples falling from trees as well as the orbits of planets around the sun. The second-most familiar force is

electromagnetism, which underlies most of the interactions in the modern technological age. Like gravity, the electric force follows an inverse square law, which means that the strength of the force varies inversely with the square of the distance between the interacting objects. With

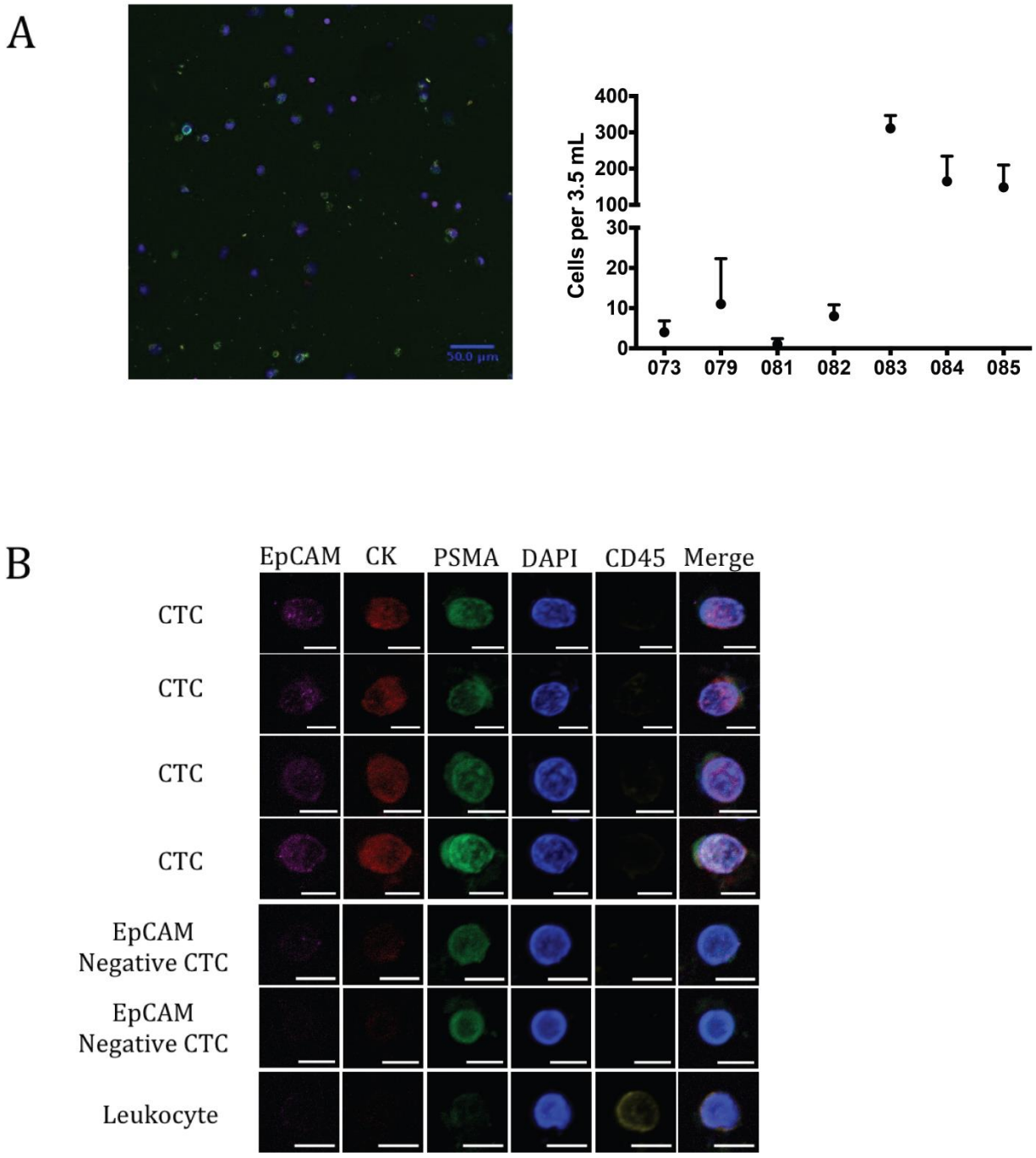

Figure 4: CTCs isolated from patient blood. Blood of patients with advanced prostate cancers was spun down to obtain buffy coat, suspended in 1% HSA and flowed through

PLL functionalized microscale flow devices. Samples were flowed through device at flow rate 0.008 mL/min (wall shear stress 0.5 dyn/cm^2). (A-B) Number of prostate cancer cells captured from flow. Following processing, captured cells were released from the microtube and plated onto 8 mm, #1.5 thickness coverslips, fixed and stained with the following: anti-CD45, anti-EpCAM, anti-PSMA (J591), anti pan-cytokeratin, and DAPI. CTCs were confirmed on basis of DAPI, cytokeratin, and CD45 staining. Only confirmed CTCs were included in final enumeration. Scale bar = 5 um.

electrically charged objects, the magnitude of the force is proportional to the product of the two charges, q_1 and q_2, divided by r^2, the square of the distance between them:

$$F = \frac{q_1}{\varepsilon}\frac{q_2}{r^2}$$

This is Coulomb's law. The constant, ε, is a property of the space between the charges and is related to the dielectric constant. In our experiments we observed negatively charged objects interacting adhesively with positively charged polymer-coated surfaces under flow conditions and, by tuning the fluid dielectric using serum albumin, we were able to modulate firm adhesion of cells based on the electric phenotype of those cells. We observed elevated electric charge in cancer cells expressing heparan sulfate proteoglycans and those cells persisted in binding to charged surfaces in high dielectric fluids. White blood cells, on the other hand, firmly adhered to cationic surfaces but the number of firmly adhered cells decreased as the fluid dielectric increased until, eventually, at 1% protein concentration, we observed almost no white blood cell adhesion. The combination of both fluid dielectric and surface charge can increase both the number and purity of CTCs isolated from patient blood, which can enable the development of effective personalized cancer therapies.

2.6 References

[1] Engberg, Anna E., Per H. Nilsson, Shan Huang, Karin Fromell, Osama A. Hamad, Tom Eirik Mollnes, Jenny P. Rosengren-Holmberg, Kerstin Sandholm, Yuji Teramura, Ian A. Nicholls, Bo Nilsson, and Kristina N. Ekdahl. "Prediction of Inflammatory Responses Induced by Biomaterials in Contact with Human Blood Using Protein Fingerprint from Plasma."*Biomaterials* 36 (2015): 55-65. Web.

[2] Lee, Ted T., José R. García, Julieta I. Paez, Ankur Singh, Edward A. Phelps, Simone Weis, Zahid Shafiq, Asha Shekaran, Aránzazu Del Campo, and Andrés J. García. "Light-triggered in Vivo Activation of Adhesive Peptides Regulates Cell Adhesion, Inflammation and Vascularization of Biomaterials." *Nature Materials Nat Mater* 14.3 (2014): 352-60. Web.

[3] Sergeeva, Yulia N., Tongtong Huang, Olivier Felix, Laura Jung, Philippe Tropel, Stephane Viville, and Gero Decher. "What Is Really Driving Cell–surface Interactions? Layer-by-layer Assembled Films May Help to Answer Questions concerning Cell Attachment and Response to Biomaterials." *Biointerphases* 11.1 (2016): 019009. Web.

[4] Mitchell, Michael J., Carlos A. Castellanos, and Michael R. King. "Surfactant Functionalization Induces Robust, Differential Adhesion of Tumor Cells and Blood Cells to Charged Nanotube-coated Biomaterials under Flow."*Biomaterials* 56 (2015): 179-86. Web.

[5] Mitchell, Michael J., Carlos A. Castellanos, and Michael R. King. "Immobilized Surfactant-nanotube Complexes Support Selectin-mediated Capture of Viable Circulating Tumor Cells in the Absence of Capture Antibodies." *Journal of Biomedical Materials Research Part A J. Biomed. Mater. Res.* 103.10 (2015): 3407-418. Web.

[6] Mitchell, Michael J., Carlos A. Castellanos, and Michael R. King. "Nanostructured Surfaces to Target and Kill Circulating Tumor Cells While Repelling Leukocytes." *Journal of Nanomaterials* 2012 (2012): 1-10. Web.

[7] Mitchell, M. J., E. Wayne, K. Rana, C. B. Schaffer, and M. R. King. "TRAIL-coated Leukocytes That Kill Cancer Cells in the Circulation."*Proceedings of the National Academy of Sciences* 111.3 (2014): 930-35. Web.

[8] Wayne, Elizabeth C., Siddarth Chandrasekaran, Michael J. Mitchell, Maxine F. Chan, Rachel E. Lee, Chris B. Schaffer, and Michael R. King. "TRAIL-coated Leukocytes That Prevent the Bloodborne Metastasis of Prostate Cancer." *Journal of Controlled Release* 223 (2016): 215-23. Web.

[9] Chandrasekaran, Siddarth, Maxine F. Chan, Jiahe Li, and Michael R. King. "Super Natural Killer Cells That Target Metastases in the Tumor Draining Lymph Nodes." *Biomaterials* 77 (2016): 66-76. Web.

[10] Sharkey, Charles C., Jiahe Li, Sweta Roy, Qianhui Wu, and Michael R. King. "Two-stage Nanoparticle Delivery of Piperlongumine and Tumor Necrosis Factor-related Apoptosis-inducing Ligand (TRAIL) Anti-cancer Therapy."*Technology TECHNOLOGY* 04.01 (2016): 60-69. Web.

[11] Essen, T.h. Van, L. Van Zijl, T. Possemiers, A.a. Mulder, S.j. Zwart, C.-H. Chou, C.c. Lin, H.j. Lai, G.p.m. Luyten, M.j. Tassignon, N. Zakaria, A. El Ghalbzouri, and M.j. Jager. "Biocompatibility of a Fish Scale-derived Artificial Cornea: Cytotoxicity, Cellular Adhesion and Phenotype, and In vivo Immunogenicity." *Biomaterials* 81 (2016): 36-45. Web.

[12] Lukas, K., U. Thomas, A. Gessner, D. Wehner, T. Schmid, C. Schmid, and K. Lehle. "Plasma Functionalization of Polycarbonaturethane to Improve Endothelialization--Effect of Shear Stress as a Critical Factor for Biocompatibility Control." *Journal of Biomaterials Applications* 30.9 (2016): 1417-428. Web.

[13] Morille, Marie, Karine Toupet, Claudia N. Montero-Menei, Christian Jorgensen, and Danièle Noël. "PLGA-based Microcarriers Induce Mesenchymal Stem Cell Chondrogenesis and Stimulate Cartilage Repair in Osteoarthritis." *Biomaterials* 88 (2016): 60-69. Web.

[14] Bagó, Juli R., Guillaume J. Pegna, Onyi Okolie, and Shawn D. Hingtgen. "Fibrin Matrices Enhance the Transplant and Efficacy of Cytotoxic Stem Cell Therapy for Post-surgical Cancer." *Biomaterials* 84 (2016): 42-53. Web.

[15] Heiden, Michael, Sabrina Huang, Eric Nauman, David Johnson, and Lia Stanciu. "Nanoporous Metals for Biodegradable Implants: Initial Bone Mesenchymal Stem Cell Adhesion and Degradation Behavior." *Journal of Biomedical Materials Research Part A J. Biomed. Mater. Res.* (2016): n. pag. Web.

[16] Cheng, Xinwei, and Robert J. Lee. "The Role of Helper Lipids in Lipid Nanoparticles (LNPs) Designed for Oligonucleotide Delivery." *Advanced Drug Delivery Reviews* 99 (2016): 129-37. Web.

[17] Marshall, Jocelyn R., and Michael R. King. "Selectin-Mediated Targeting of Circulating Tumor Cells for Isolation and Treatment." *Isolation and Analysis Circulating Tumor Cells* (2016): 267-86. Web.

[18] Hughes, Andrew D., Graham Marsh, Richard E. Waugh, David G. Foster, and Michael R. King. "Halloysite Nanotube Coatings Suppress Leukocyte Spreading." *Langmuir* 31.50 (2015): 13553-3560. Web.

[19] García-Recio, Eva M., Celia Pinto-Díez, M. Isabel Pérez-Morgado, Marta García-Hernández, Gerónimo Fernández, M. Elena Martín, and Víctor M. González. "Characterization of MNK1b DNA Aptamers That Inhibit Proliferation in MDA-MB231 Breast Cancer Cells." *Molecular Therapy—Nucleic Acids Mol Ther Nucleic Acids* 5.1 (2016): n. pag. Web.

[20] Minasyan, Hayk. "Mechanisms and Pathways for the Clearance of Bacteria from Blood Circulation in Health and Disease." *Pathophysiology* (2016): n. pag. Web.

[21] Hondroulis, Evangelia, Rui Zhang, Chengxiao Zhang, Chunying Chen, Kosuke Ino, Tomokazu Matsue, and Chen-Zhong Li. "Immuno Nanoparticles Integrated Electrical Control of Targeted Cancer Cell Development Using Whole Cell Bioelectronic Device." *Theranostics* 4.9 (2014): 919-30. Web.

[22] Szachowicz-Petelska, Barbara, Izabela Dobrzyska, Stanisaw Sulkowski, and Zbigniew A. "Characterization of the Cell Membrane During Cancer Transformation." *Colorectal Cancer Biology - From Genes to Tumor*(2012): n. pag. Web.

[23] Dobrzyńska, Izabela, Elżbieta Skrzydlewska, and Zbigniew A. Figaszewski. "Changes in Electric Properties of Human Breast Cancer Cells." *J Membrane Biol The Journal of Membrane Biology* 246.2 (2012): 161-66. Web.

[24] Porel, Mintu, and Christopher A. Alabi. "Sequence-Defined Polymers via Orthogonal Allyl Acrylamide Building Blocks." *J. Am. Chem. Soc. Journal of the American Chemical Society* 136.38 (2014): 13162-3165. Web.

[25] Pack, Daniel W., Allan S. Hoffman, Suzie Pun, and Patrick S. Stayton. "Design and Development of Polymers for Gene Delivery." *Nature Reviews Drug Discovery Nat Rev Drug Discov* 4.7 (2005): 581-93. Web.

[26] Sigal, George B., Milan Mrksich, and George M. Whitesides. "Effect of Surface Wettability on the Adsorption of Proteins and Detergents." *J. Am. Chem. Soc. Journal of the American Chemical Society* 120.14 (1998): 3464-473. Web.

[27] Lvov, Yuri, Katsuhiko Ariga, Izumi Ichinose, and Toyoki Kunitake. "Assembly of Multicomponent Protein Films by Means of Electrostatic Layer-by-Layer Adsorption." *J. Am. Chem. Soc. Journal of the American Chemical Society* 117.22 (1995): 6117-123. Web.

[28] Gessner, Andrea, Antje Lieske, Bernd R. Paulke, and Rainer H. Müller. "Influence of Surface Charge Density on Protein Adsorption on Polymeric Nanoparticles: Analysis by Two-dimensional Electrophoresis."*European Journal of Pharmaceutics and Biopharmaceutics* 54.2 (2002): 165-70. Web.

[29] Rose, Susanna F., Andrew L. Lewis, Geoffrey W. Hanlon, and Andrew W. Lloyd. "Biological Responses to Cationically Charged Phosphorylcholine-based Materials in Vitro." *Biomaterials* 25.21 (2004): 5125-135. Web.

[30] Saha, Krishnendu, Mehran Rahimi, Mahdieh Yazdani, Sung Tae Kim, Daniel Moyano, Singyuk Hou, Riddha Das, Rubul Mout, Farhad Rezaee, Morteza Mahmoudi, and Vincent M. Rotello. "Regulation of Macrophage Recognition through the Interplay of Nanoparticle Surface Functionality and Protein Corona." *ACS Nano* (2016): n. pag. Web.

[31] Stan, Claudiu A., Sindy K. Y. Tang, Kyle J. M. Bishop, and George M. Whitesides. "Externally Applied Electric Fields up to 1.6 × 10 5 V/m Do Not Affect the Homogeneous Nucleation of Ice in Supercooled Water."*The Journal of Physical Chemistry B J. Phys. Chem. B* 115.5 (2011): 1089-097. Web.

[32] *Philosophiae Naturalis Principia Mathematica* ("*Mathematical Principles of Natural Philosophy*"), London, 1687; Cambridge, 1713; London, 1726. *Isaac Newton's Philosophiae Naturalis Principia Mathematica, the Third Edition with Variant Readings,* ed. A. Koyré and I. B. Cohen, 2 vols., Cambridge: Harvard University Press and Cambridge: Cambridge University Press, 1972. *The Principia: Mathematical Principles of Natural Philosophy: A New Translation*, tr. I. B. Cohen and Anne Whitman, preceded by "A Guide to Newton's*Principia*" by I. B. Cohen, Berkeley: University of California Press, 1999.